Healthy cells functionally present TAP-independent SSR1 peptides: implications for selection of clinically relevant antigens

Waard, A.A. de; Verkerk, T.; Hoefakker, K.; Steen, D.M. van der; Jongsma, M.L.M.; Kadosh, D.M.; ... ; Spaapen, R.M.
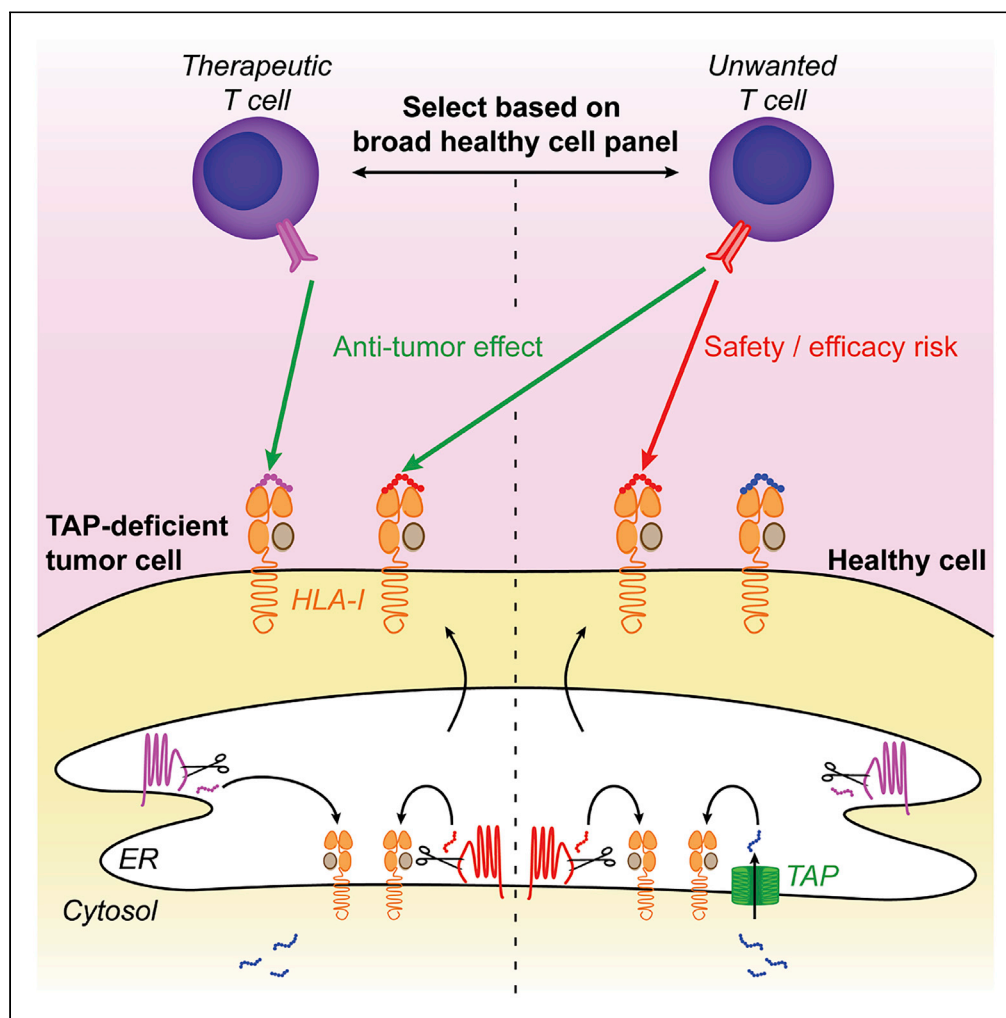
Article

Healthy cells functionally present TAP-independent SSR1 peptides: implications for selection of clinically relevant antigens

Antonius A. de Waard, Tamara Verkerk, Kelly Hoefakker, ..., Marieke Griffioen, Mirjam H.M. Heemskerk, Robbert M. Spaapen

r.spaapen@sanquin.nl

HIGHLIGHTS

The ER-resident SSR1 holds an antigenic peptide that is processed independently of TAP

TAP-independent peptide presentation is functional in healthy cell types

TAP-independent SSR1-derived antigen presentation varies between healthy cells

This exposes safety and efficacy risks of clinical TAP-independent peptide targeting

Article

Healthy cells functionally present TAP-independent SSR1 peptides: implications for selection of clinically relevant antigens

Antonius A. de Waard,[1,2,7] Tamara Verkerk,[1,2,7] Kelly Hoefakker,[1,2] Dirk M. van der Steen,[3] Marlieke L.M. Jongsma,[1,2,4] Dganit Melamed Kadosh,[5] Sophie Bliss,[1,2] Arnoud H. de Ru,[6] Arie Admon,[5] Peter A. van Veelen,[6] Marieke Griffioen,[3] Mirjam H.M. Heemskerk,[3] and Robbert M. Spaapen[1,2,8,*]

SUMMARY

Tumors with an impaired transporter associated with antigen processing (TAP) present several endoplasmic reticulum-derived self-antigens on HLA class I (HLA-I) which are absent on healthy cells. Selection of such TAP-independent antigens for T cell-based immunotherapy should include analysis of their expression on healthy cells to prevent therapy-induced adverse toxicities. However, it is unknown how the absence of clinically relevant antigens on healthy cells needs to be validated. Here, we monitored TAP-independent antigen presentation on various healthy cells after establishing a T cell tool recognizing a TAP-independent signal sequence receptor 1-derived antigen. We found that most but not all healthy cells present this antigen under normal and inflammatory conditions, indicating that TAP-independent antigen presentation is a variable phenomenon. Our data emphasize the necessity of extensive testing of a wide variety of healthy cell types to define clinically relevant TAP-independent antigens that can be safely targeted by immunotherapy.

INTRODUCTION

HLA class I (HLA-I) (neo)antigen presentation by tumor cells can induce activation of CD8^{+} cytotoxic T cells (Neefjes et al., 2011). This natural immunological pressure forces various tumors to downmodulate HLA-I antigen presentation through genomic or epigenetic alterations (Campoli and Ferrone, 2008; Khong and Restifo, 2002). In addition, T cell-based immunotherapies increase mutation rates in genes associated with antigen presentation such as *B2M*, *tapasin*, *TAP1*, and *TAP2* (Gettinger et al., 2017; Jiang et al., 2010; Restifo et al., 1996; Sade-Feldman et al., 2017).

HLA-I is generated and folded in the ER, assisted by several lectin chaperones and stabilized by the beta-2 microglobulin (B2M) light chain, enabling the loading of small peptides through the collaborative effort of tapasin, calreticulin, and ERp57 (Rock et al., 2016). Conventional peptide generation is mediated by the proteasome in the cytosol. These peptides are transported into the endoplasmic reticulum (ER) by the heterodimeric transporter associated with antigen processing (TAP) complex.

Alterations in the antigen presentation machinery affect the composition of the peptide repertoire presented by HLA-I (van Hall et al., 2006). Perhaps the largest impact on the repertoire is the functional disruption of the TAP transporter (hereafter referred to as TAP-deficient), interrupting the supply of cytosolic peptides. Without TAP, HLA-I presented peptides are either derived from ER-resident proteins or enter the ER through routes other than the canonical TAP pathway (Oliveira and van Hall, 2015). Several of these so-called TAP-independent peptides are not presented on healthy TAP-proficient cells, therefore representing a potential specific immunotherapeutic target on TAP-deficient tumors (van Hall et al., 2006). Since studies targeting TAP-independent peptides in mice show low toxicity, the first proof-of-concept study targeting TAP-independent peptides in patients with non-small cell lung cancer will soon be initiated (Brolsma, 2019; Doorduijn et al., 2018). Potential target antigens for such therapy were recently identified in humans by comparing the HLA-I presented peptidome eluted from TAP-deficient and -proficient cells (Marijt et al., 2018). Because a considerable proportion of TAP-independent peptides can also be presented by at least some TAP-proficient cells (Man et al., 1992; Weinzierl et al., 2008), clinical targeting of

[1]Department of Immunopathology, Sanquin Research, Amsterdam, CX 1066, The Netherlands

[2]Landsteiner Laboratory, Amsterdam UMC, University of Amsterdam, Amsterdam, CX 1066, The Netherlands

[3]Department of Hematology, LUMC, Leiden, ZA 2333, The Netherlands

[4]Oncode Institute and Department of Cell and Chemical Biology, LUMC, Leiden, ZA 2333, The Netherlands

[5]Faculty of Biology, Technion–Israel Institute of Technology, Haifa 32000, Israel

[6]Center for Proteomics and Metabolomics, LUMC, Leiden, ZA 2333, The Netherlands

[7]These authors contributed equally

[8]Lead contact

*Correspondence: r.spaapen@sanquin.nl

https://doi.org/10.1016/j.isci.2021.102051

TAP-independent antigens potentially involves significant safety and efficacy risks. Although caution is needed in designating peptides as solely being presented on TAP-deficient cells, efforts are largely lacking to validate that antigens are not at all presented by any healthy cell type with native TAP expression.

To define a validation roadmap, it would be instrumental to have a tool—such as a defined T cell clone—to monitor functional TAP-independent peptide presentation both on tumor and healthy cells. However, isolation of T cells targeting TAP-independent antigens on healthy cells may be challenging since they are likely deleted during thymic development (Takaba and Takayanagi, 2017). Therefore, human T cells that recognize a molecularly defined TAP-independent antigen on healthy cells have not been identified to date.

To bypass potential thymic deletion issues, we here investigated TAP-independent antigen recognition on healthy cells using CD8^{+} T cell clones derived from allogeneic repertoires (Amir et al., 2011; Van Bergen et al., 2010). We identified that the cognate antigen of one of these clones, derived from the ER-resident protein signal sequence receptor 1 (SSR1), is presented both by TAP knockout (KO) and TAP-proficient tumor cells. This ubiquitously expressed antigen is effectively presented under normal and inflammatory conditions on several but not all healthy primary cells, indicating that TAP-independent antigen presentation is a variable phenomenon. Thus, a broad healthy cell expression analysis of TAP-independent targets improves the safety profile of their immunotherapeutic application.

RESULTS

The protein SSR1 encodes a TAP-independent peptide

To study the effect of the TAP transporter on the functional presentation of antigens, we genetically knocked out TAP1 in human HAP1 cells. After lentiviral introduction of CRISPR/Cas9 machinery targeting the first exon of *TAP1*, 20% of the transduced cells still displayed surface HLA-I levels comparable to wild type cells (Figures 1A and S1). In order to prevent interference of remaining wild-type cells in T cell coculture assays, we generated five clonal TAP1 KO cell lines which showed decreased HLA-I surface expression (Figure 1B). In addition, Western blot analysis confirmed a complete lack of TAP1 expression in clone #1 (de Waard et al., 2020). Sequence analyses showed a lack of at least one amino acid in the first transmembrane domain of TAP1 in each clone (Figures S2A and S2B) (Schrodt et al., 2006).

To analyze functional presentation of antigens in the absence of the TAP transporter, we utilized several available alloreactive CD8^{+} T cell clones that we previously isolated from patients following allogeneic stem cell transplantation (Amir et al., 2011; Van Bergen et al., 2010). These T cell clones recognize defined antigens, one of which is derived from the ER-localized protein SSR1 and may therefore be processed independently of TAP-mediated cytosol-to-ER transport (Pfeffer et al., 2017). Two other T cell clones recognize antigens derived from the cytosolic proteins USP11 or VPS13B (Koike and Jahn, 2019; Zhou et al., 2017). Since these antigens are presented by HLA-A2, we first confirmed that this specific allele was affected in the TAP1 KO cells (Figure 1C). Subsequent coculture of T cells with HAP1 target cells showed that USP11- and VPS13B-specific T cells recognized wild type but not TAP-deficient cells (Figure 1D, right panels). Conversely, SSR1-specific T cells were activated by the TAP-deficient cells demonstrating that the SSR1 peptide is processed independently of TAP (Figure 1D, left panel). The amount of HLA-A2 on the different TAP1 KO clones (Figure 1C) did not correlate with their capacity to stimulate SSR1-specific T cells (Figure S2C). Strikingly, HAP1 wild-type cells were capable of activating SSR1-specific T cells to a similar level as TAP-deficient cells resulting in T cell-mediated lysis of both cell lines, showing that the SSR1 peptide can be functionally presented at the cell surface even in the presence of the TAP transporter (Figures 1D and 1E). Thus, the SSR1 peptide represents a model antigen to further evaluate TAP-independent antigen presentation by healthy cells.

The SSR1 signal peptide contains the TAP-independent SSR1 antigen

SSR1 is the transmembrane spanning alpha subunit of the TRAP complex that translocates proteins co-translationally in the ER lumen (Pfeffer et al., 2017). The epitope recognized by the SSR1-specific T cell clone is polymorphic in the population as dictated by a nonsynonymous SNP (rs10004) encoding for either a serine or leucine (SSR1-S of SSR1-L) (Figure S3) (Van Bergen et al., 2010). A 14-mer peptide containing this polymorphism (VLFRGGPRGSLAVA) was previously shown to be presented by HLA-A2 and recognized by SSR1-specific T cells, albeit with low avidity (Bijen et al., 2018). As more specific details on functionally presented SSR1 antigens may aid in defining TAP-independent peptide processing, we next investigated the HLA-I mediated presentation and recognition of additional peptides covering the SNP. *In silico*
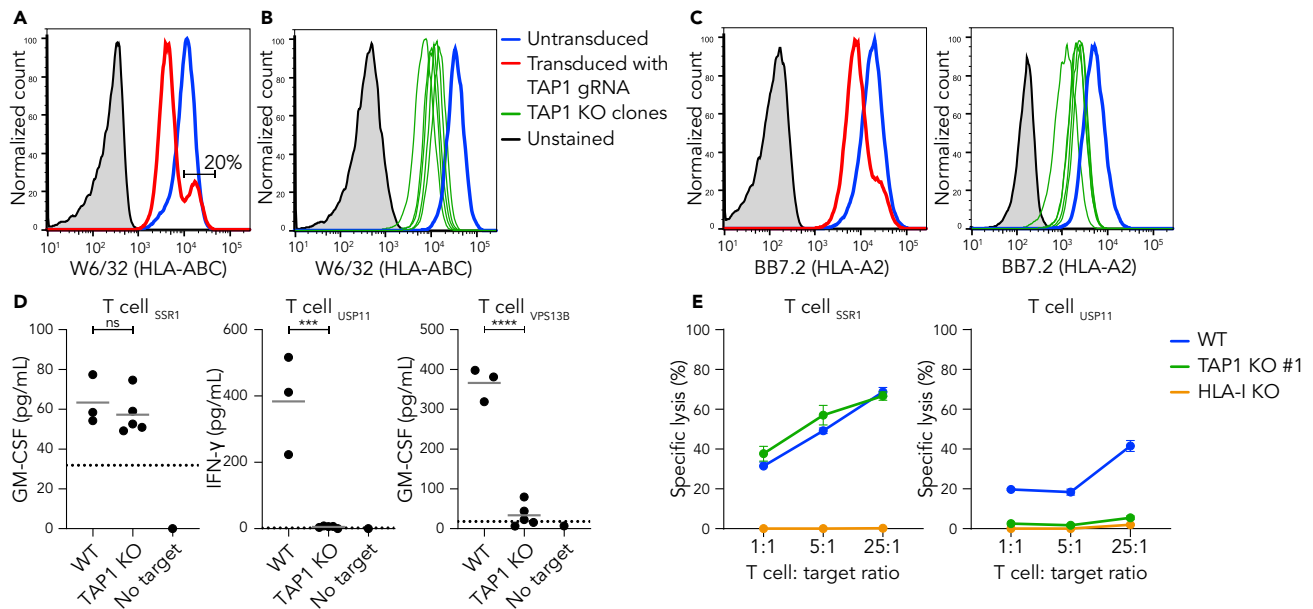
Figure 1. The protein SSR1 encodes a TAP-independent peptide

(A) HAP1 cells were transduced with a TAP1-specific gRNA and analyzed by flow cytometry using the pan-HLA antibody W6/32. Untransduced (blue), transduced (red) and unstained cells (gray). See Figure S1 for gating strategy.

(B) Five monoclonal cell lines were generated from the polyclonal TAP1 KO cell line in (A) and analyzed by flow cytometry. Wild-type (blue), TAP1 KO clones (green lines), unstained cells (gray). See Figure S2 for sequencing details.

(C) Same as (A) and (B) but using the HLA-A2-specific antibody BB7.2.

(D) HLA-A2-restricted SSR1-, USP11- or VPS13B-specific T cells were cocultured with three separate batches of HAP1 wild-type or each of the five clonal TAP1 KO cell lines (B) (Amir et al., 2011; Pont et al., 2019; Spaapen et al., 2007, 2008; Van Bergen et al., 2010). Culture supernatant was used for indicated cytokine ELISAs. Each datapoint represents the average of triplicate cultures. Dotted lines represent the lower detection limit of the ELISA. Student's t-test, ***p < 0.001, ****p < 0.0001, ns is not significant.

(E) The indicated T cells were cocultured with ^{51}Cr-loaded wild-type, TAP1 KO #1 and HLA-I KO HAP1 cells (Jongsma et al., 2020) at indicated effector:target cell ratios, after which specific lysis (%) was calculated based on ^{51}Cr release. Each datapoint represents the mean of triplicate cultures with SD.
See also Figures S1 and S2.

HLA-A2-binding predictions of SSR1 peptides covering the SNP failed to designate strong binders (Table S1). Since predictions for this SSR1 epitope can be inaccurate (Bijen et al., 2018), we biochemically determined whether SSR1 peptides other than the 14-mer are presented by HLA-A2 positive cells. Using LC-MS/MS we analyzed eluted peptides from HAP1 wild-type cells (de Waard et al., 2020), and from two HLA-A2 positive primary AML samples that genetically encode the SSR1-S peptide. In first instance, we automatically retrieved only SSR1-L peptides (13-mer and 14-mer) from the AML samples (Table 1). In addition, using the MS2 spectrum of a synthetic SSR1-S 14-mer peptide as reference, we identified this peptide in all three samples (Table 1).

To obtain more data on presented SSR1-derived peptides, we analyzed the peptidome from additional HLA-A2 positive primary tumor samples (n = 9) and cell lines (n = 6). As both SSR1-S and SSR1-L are presented at similar levels by HLA-A2 positive cells (Bijen et al., 2018), we further focused on identifying length variants of the SSR1-L peptide. The analysis yielded four length variants of the same core peptide (VLFRGGPRGLL*AVA*) covering the polymorphic residue (Table 2). Coculture of SSR1-specific T cells with S-antigen-negative T2 cells loaded with decreasing amounts of synthetic candidate peptides showed superior responses against the 14-mer peptide (Figure 2A). These data establish the 14-mer peptide as the cognate epitope of the SSR1-specific T cell clone.

The location of an antigen within a transmembrane protein determines the molecular path of presentation, including the requirement for TAP transportation after proteolytic degradation (Oliveira and van Hall, 2013). SSR1 is a type-I transmembrane protein with an intra-ER domain of 189 amino acids and a cytosolic domain of 58 amino acids (Pfeffer et al., 2017). To gain insight into the presentation route of the SSR1 antigen, we analyzed the subcellular localization of the recognized peptide. The 14-mer peptide is located near the N-terminus of the

Table 1. Immunopeptidome analyses of cells genetically positive for SSR1-S

Candidate peptide	Identified on	Genotype rs10004	Predicted affinity for HLA-A*02:01 (nM)
VLFRGGPRG**S**LAVA	HAP1, AGP2375, SWD2031	S/S, S/L, S/L	1403
VLFRGGPRG**L**LAVA	AGP2375	S/L	649
VLFRGGPRG**L**LAV	SWD2031	S/L	236

SSR1-S and SSR1-L candidate peptides were eluted from HAP1 cells and two primary AMLs (Hassan et al., 2013; van der Lee et al., 2019). Affinities for HLA-A*02:01 were predicted using NetMHC4.0. See also Table S1.

SSR1 protein, spanning part of the H- and the complete C-region of the signal peptide as predicted by Phobius (Kall et al., 2007) and is likely to be C-terminally liberated in the ER by the signal peptidase complex (Figures 2B and S3) (Voldby Larsen et al., 2006; Weinzierl et al., 2008). In summary, the peptides derived from USP11 and VPS13B require TAP translocation before HLA-I binding, whereas the SSR1 peptide is readily localized in the ER and likely processed by local proteases before being loaded on HLA-I (Figure 2C).

Multiple SSR1 peptides are presented independently of TAP

To establish whether other HLA-I alleles can also present TAP-independent SSR1 peptides, we analyzed the peptidomes of TAP-deficient HAP1 cells and MCF-7 cells expressing the herpes simplex virus TAP inhibitor infected cell protein 47 (ICP47). These analyses confirmed that the antigen recognized by our SSR1-specific T cell clone was presented by TAP-deficient HAP1 cells (Table S2). In addition, we identified two SSR1-derived candidate peptides from TAP-inhibited MCF-7 cells, indicating that other SSR1 antigens may also be presented independently of TAP (Table S2 and Figure S3). Because these candidate peptides were also found on wild-type MCF-7 cells (Table S2), we questioned whether even more ER-derived SSR1 peptides can be presented by TAP-proficient cells. Examination of membrane bound and soluble HLA-I presented peptidomes from cells and sera of glioblastoma patients and non-cancerous individuals revealed multiple SSR1-derived candidate peptides (Table S3) (Shraibman et al., 2019). All candidate peptides were derived from the ER-luminal domain of SSR1 (Figure S3).

Altogether, the identification of a vast number of ER-derived SSR1 candidate peptides presented by a variety of HLA-I alleles on different cells (Tables 1 and 2, S2, and S3) indicates that multiple TAP-independent peptides derived from a single protein can be presented by TAP-proficient cells.

TAP-independent peptide presentation is functional in healthy donor cells

To investigate the capacity of non-transformed cells to present TAP-independent peptides, we determined the reactivity of the SSR1-specific T cell clone against healthy donor material. Monocytes, T cells and B cells, the main constituents of peripheral blood mononuclear cells (PBMCs), express SSR1 according to publicly available RNA-seq data (Figure 3A). Therefore, we isolated PBMCs from three HLA-A2 positive healthy donors and genotyped rs10004 to evaluate whether these donors were carrying the antigen recognized by the SSR1-specific T cell clone. Two donors (A and B) were heterozygous for rs10004 and thus positive for the SSR1 epitope, and one donor (C) was homozygous negative (Figure 3B). Coculture of our T cell clones with fresh PBMCs from the three donors largely failed to elicit a detectable response of SSR1-specific T cells toward antigen positive donors, while the positive control USP11- and VPS13B-specific clones were activated (Figures 3C and S4A). In contrast, monocytes isolated from the genetically positive PBMCs induced an SSR1-directed T cell response (Figures 3D and S4B). We then interrogated T cell reactivity against human umbilical cord endothelial cells (HUVECs), as a non-hematopoietic healthy cell type that expresses SSR1 (Figure 3E and S4C). SSR1-specific T cells recognized and killed selected HLA-A2 positive, SSR1-antigen positive HUVECs, but not HLA-A2 negative control HUVECs (Figures 3F, 3G, and S4D). Together, these data demonstrate that presentation of the TAP-independent SSR1-antigen is functional in multiple but not all healthy TAP-proficient cells.

TAP-independent peptides are presented under inflammatory conditions

Patients receiving immunotherapy regularly experience severe inflammatory reactions and cytokine storm, which may also be the case after immunotherapeutic targeting of TAP-independent peptides (Gangadhar

Table 2. Immunopeptidome analysis reveals seven candidate peptides covering the SSR1 SNP (rs10004)

Candidate peptide	Identified from			Predicted affinity for HLA-A*02:01 (nM) per variant	
	Primary tumor	Cell line	TAP-deficient cell line	L	S
VLFRGGPRG**LL**	–	–	T2	4673	5524
VLFRGGPRG**LL**A	OvaL10	UM9+ A2	–	5795	10,082
VLFRGGPRG**LL**AV	SWD2031	–	–	236	628
VLFRGGPRG**LL**AVA	AGP2375, CDT4512, KYE9115, OvaL10, OvaL23, GBZ10197, GPQ3361, VDL6711, ALY1143	U266, TMD8+A2, COV413b, U2G10196, UM9+A2	T2	649	1403

SSR1-L candidate peptides eluted from different primary tumors (anonymized patient numbers indicated) and cell lines. Affinities for HLA-A*02:01 were predicted using NetMHC4.0 for both SSR1-L and SSR1-S of rs10004. See also Tables S1–S3 (Komov et al., 2018).

and Vonderheide, 2014; Hay et al., 2017; Henden and Hill, 2015). Inflammatory cytokines such as IFN-γ enhance expression of various components of the HLA-I pathway including the TAP transporter, but their influence on the expression and presentation of the antigens studied here is unknown (Jongsma et al., 2019; Ma et al., 1997). Therefore, we first analyzed the change in expression of SSR1, USP11, and VPS13B after 24 hr of IFN-γ treatment using microarray datasets from the Interferome database (Rusinova et al., 2012). In comparison to the reference gene *PPIA* (Riemer et al., 2012), the expression of *SSR1, USP11* and *VPS13B* were unaffected by IFN-γ treatment, whereas *TAP1* and *TAP2* expression were increased (Figure 4A). Additionally, proteome analysis after 48 hr IFN-γ stimulation revealed no significant change in SSR1 and USP11 protein levels while TAP1 and TAP2 increased eight-fold (Figure 4B) (Megger et al., 2017).

To examine the effects of inflammatory conditions on TAP-independent peptide presentation, we stimulated HAP1 wild-type and TAP1 KO cells for 48 hr with IFN-γ, which resulted in increased HLA-A2 surface expression on both cell types (Figure 4C). These stimulated cells and their unstimulated controls were then exposed to the different T cell clones. The IFN-γ-induced upregulation of classical antigen presentation on wild type cells was characterized by an increased T cell response against control USP11 and VPS13B peptides (Figure 4D, right panels). These IFN-γ stimulated wild-type cells also presented significant amounts of SSR1 peptide (Figure 4D, left panel). In addition, the SSR1 peptide presentation in the absence of the TAP transporter was similar after IFN-γ stimulation (Figure 4D). These results indicate that this TAP-independent antigen presentation pathway is largely unaffected by an inflammatory IFN-γ stimulus on an immortal model cell line.

Activated healthy cells functionally present TAP-independent peptides

To evaluate whether healthy tissues present TAP-independent peptides under inflammatory conditions similar as induced by immunotherapy, we evaluated recognition of the TAP-independent SSR1 antigen on activated healthy cells. Although functional SSR1 antigen presentation by unstimulated PBMCs was negligible (Figure 3C), we observed a significant SSR1-specific T cell response against IFN-γ treated PBMCs from the SSR1 antigen-positive donors A and B but not against the antigen-negative donor C (Figure 5A). In order to test the TAP-independent antigen presentation in a broader inflammatory context, we activated B cells of the same three donors using CpG and a BCR-stimulus. The antigen-positive activated B cells were efficiently recognized and killed by SSR1-specific T cells, further substantiating that an inflammatory environment allows for TAP-independent antigen presentation in healthy cells (Figures 5B and S4E). Finally, the SSR1-specific T cells were also reactive to non-immune cells (HUVECs) pre-exposed to IFN-γ
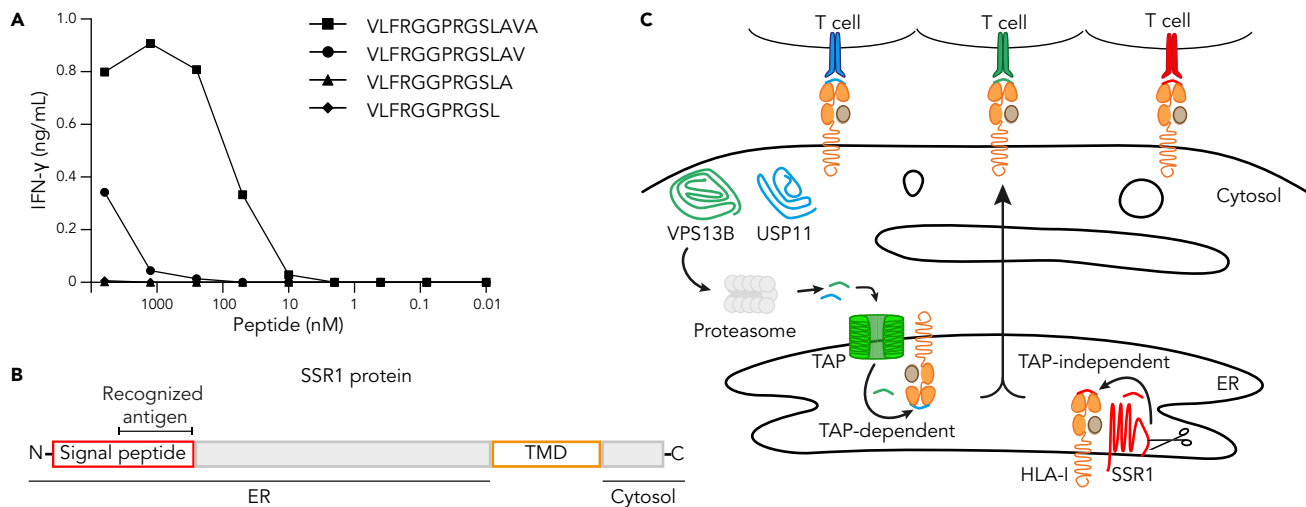
Figure 2. The SSR1 signal peptide contains the TAP-independent SSR1 antigen

(A) T2 cells, loaded with different amounts of synthetic length variants of the SSR1-S peptide (peptide sequences in Table 2), were cocultured with SSR1-specific T cells after which culture supernatant was used for IFN-γ ELISA. Each datapoint represents a single measurement.

(B) Summary of the location of the antigenic peptide in the SSR1 protein. TMD, transmembrane domain (yellow).

(C) Graphic summary of subcellular localization of the three parental proteins studied here and the presumed pathway of their antigenic peptides for presentation on HLA-I to their cognate T cells.

See also Figure S3.

(Figure 5C). Together, our data demonstrate that healthy TAP-proficient cells can efficiently present TAP-independent peptides under steady state and inflammatory conditions.

DISCUSSION

Tumor-specific abrogation of the antigen presentation machinery can provide opportunities for new therapeutic approaches, such as targeting (neo)antigens that are presented only in the case of a defective TAP transporter (Marijt and van Hall, 2020; Oliveira and van Hall, 2013; van Hall et al., 2006). In our current study, we identified that an immunogenic T cell epitope originating from the ER-resident protein SSR1 is processed independently of TAP. Using an SSR1-specific T cell clone, we provide evidence that TAP-independent presentation is variable on various healthy cell types under resting and inflammatory conditions. Thus, to ensure the safety and efficacy of a therapy against TAP-independent antigens, our data imply that it is vital for every individual target to map the degree of presentation on healthy tissue.

Therapeutic targeting of non-mutated TAP-independent antigens has potential for broad clinical application, since these antigens are shared among patients with TAP-deficient tumors (Oliveira et al., 2013; van Hall et al., 2006; Voldby Larsen et al., 2006). Such immunotherapies will utilize either vaccination strategies or adoptive transfer of specific T cells. A strict prerequisite for a vaccination strategy to be effective is the lack of presentation of the targeted antigen(s) on healthy cells because otherwise specific T cells will be functionally impaired or deleted during thymic development (Doorduijn et al., 2016; Takaba and Takayanagi, 2017). Importantly, such immune tolerance inherently provides a safety margin for clinical studies in which presentation of targeted antigens would unexpectedly be not restricted to TAP-deficient cells. To increase the chance of raising an effective immune response against TAP-independent antigens, vaccination with TAP-silenced DCs could be a potential strategy (Marijt et al., 2019). Of note, there are multiple reports that in humans vaccination strategies against antigens presented on healthy tissue can break tolerance and induce severe autoimmunity, so caution is warranted (Ludewig et al., 2000; Sultan et al., 2017). The alternative for immunotherapeutic vaccination is adoptive T cell transfer, which can induce a fast anti-tumor response. A combination of adoptive transfer of T cells specific for a tumor-restricted TAP-independent antigen with repeated long peptide vaccination proved effective against murine TAP-deficient tumors (Doorduijn et al., 2016). However, presentation of a target antigen by only a subset of healthy cells can induce lethal autoimmune toxicity (Cameron et al., 2013; Morgan et al., 2013; Yee et al., 2000). Our study emphasizes that TAP-independent peptides may be presented by a subset of TAP-proficient cells. Thus, before clinical targeting of TAP-independent antigens, it is crucial to apply a thorough selection with the goal to exclude antigens that are presented on healthy cells.
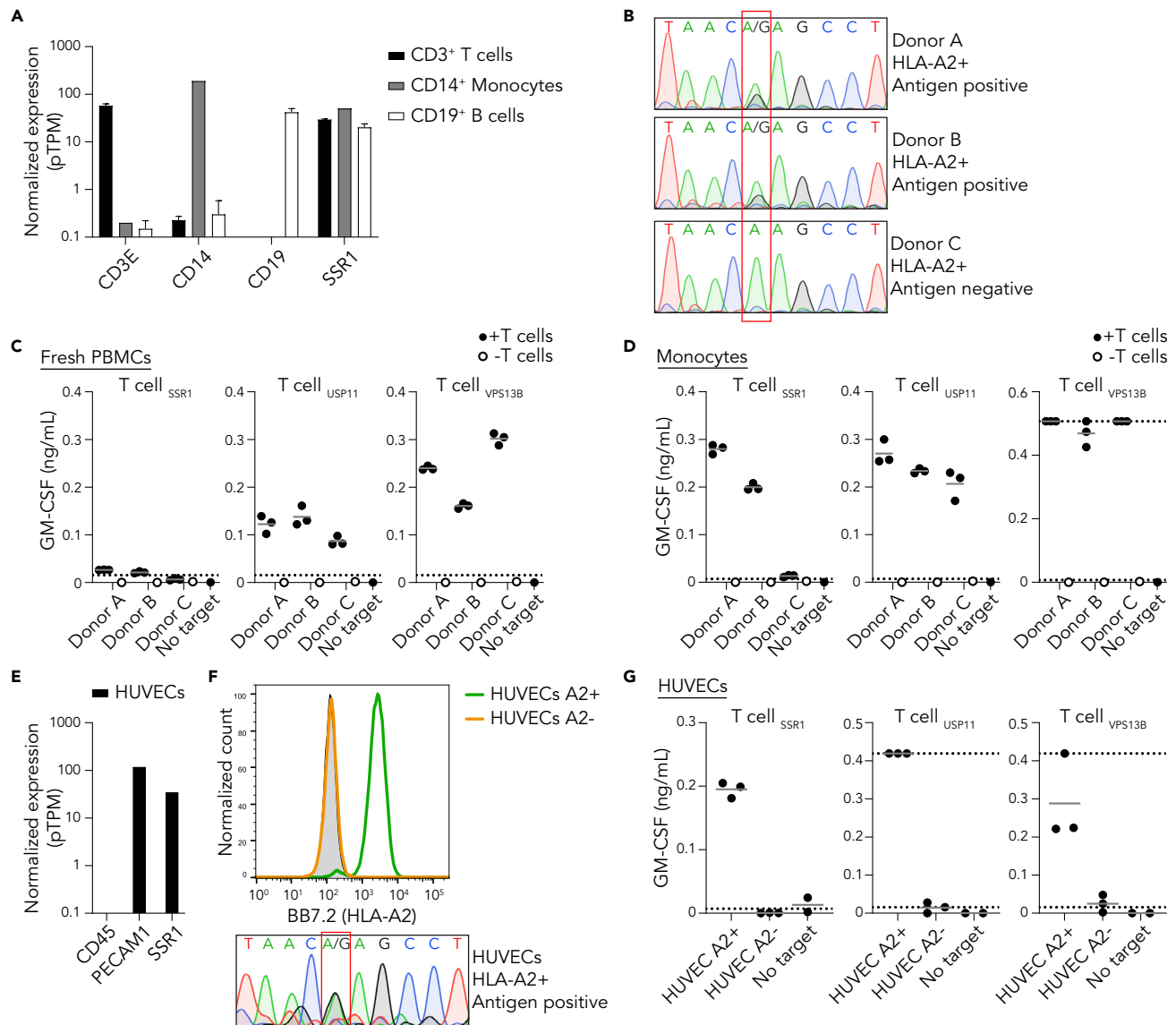
Figure 3. TAP-independent peptide presentation is functional in healthy donor cells

(A) Normalized expression of SSR1 and control CD14, CD19, and CD3E per depicted PBMC subset using the RNA HPA blood cell gene data (Uhlen et al., 2015). Data are represented as mean with SD.

(B) Sanger sequencing of the SSR1 SNP rs10004 of three HLA-A2 positive healthy donors, the position of the SNP is highlighted by the red box and consequence for antigen status is depicted.

(C) T cell coculture with PBMCs from three healthy donors (B), culture supernatant was analyzed by GM-CSF ELISA (IFN-γ data in Figure S4). Results from triplicate cultures are shown. Dotted lines represent the detection limits of the ELISA.

(D) As in (C) but using monocytes as target cells (IFN-γ data in Figure S4).

(E) Expression analysis of SSR1 and control CD45 and PECAM1 in TERT2 immortalized HUVECs using the RNA HPA cell line gene data.

(F) Flow cytometric analysis of HLA-A2 expression by HUVECs. HLA-A2 positive FACS sorted (green), HLA-A2 negative FACS sorted (orange) populations and unstained HUVECs (gray). Lower panel depicts rs10004 sequence of the HLA-A2 positive sorted HUVECs.

(G) T cell coculture with HLA-A2 positive and negative HUVECs (F). Culture supernatant was analyzed by GM-CSF ELISA (IFN-γ data in Figure S4). Each dot represents an individual measurement of triplicate cultures.

See also Figures S1 and S4.

To optimally select target antigens, mechanistic insights into the intracellular process of peptide selection are required. Current knowledge on how certain TAP-independent peptides fail to be selected for presentation in the presence of TAP is limited. Hypotheses are based on the peptide affinity for HLA-I, its abundance in the ER, and the distance between generation site and peptide-receptive HLA-I molecules
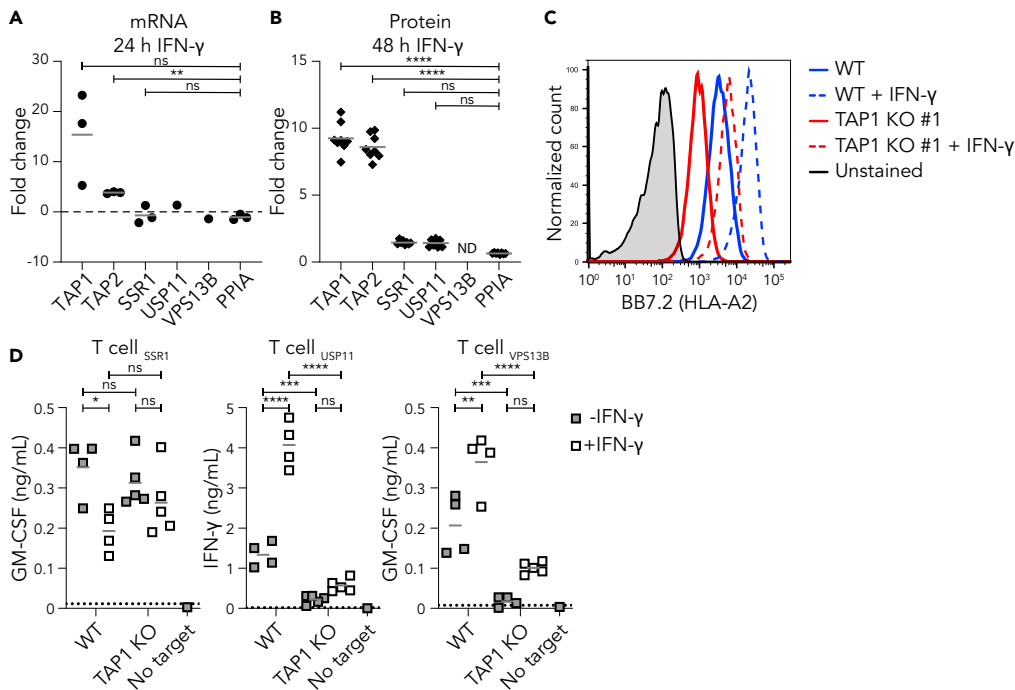
Figure 4. TAP-independent peptides are presented under inflammatory conditions

(A) *TAP1*, *TAP2*, *SSR1*, *USP11*, and *VPS13B* mRNA expression after 24 hr of IFN-γ stimulation was analyzed using three publicly available datasets and compared to the reference gene *PPIA*.

(B) TAP1, TAP2, SSR1, USP11, and VPS13B protein expression after 48 hr of IFN-γ stimulation was analyzed using publicly available MS data and compared to the reference protein PPIA (Megger et al., 2017). ND is not detected.

(C) HAP1 wild-type and TAP1 KO cells were treated with IFN-γ for 48 hr and surface HLA-A2 upregulation was measured by flow cytometry. Unstimulated (solid) or stimulated (dashed) wild type (blue) and TAP1 KO #1 (red) cells are shown, including unstimulated unstained wild type cells (gray).

(D) T cell coculture with unstimulated or IFN-γ stimulated wild-type or TAP1 KO clones (same as in Figure 1B). Culture supernatants were analyzed for the presence of cytokines using cytokine ELISA. Dotted lines represent the lower and upper detection limits of the ELISA. Repeated measures one-way ANOVA followed by Dunnett's (A), ordinary one-way ANOVA followed by Dunnett's (B) or by Sidak's (D) multiple comparisons test. *p < 0.05, **p < 0.01, ***p < 0.001, ****p < 0.0001, ns is not significant.

See also Figure S1.

(Durgeau et al., 2011; Oliveira et al., 2011; Oliveira and van Hall, 2013). Our human TAP-independent SSR1 antigen and its cognate T cells represent a unique toolset to further investigate existing and novel hypotheses. In support of the affinity hypothesis, the 14-mer SSR1 peptide, which has an HLA-A2 affinity well below the generally accepted threshold for presentation of 500 nM (78 nM), is selected for presentation in the presence of TAP (Bijen et al., 2018; Paul et al., 2013). However, several TAP-independent peptides that are not presented by a TAP-proficient model cell line have a strong predicted HLA-I binding, suggesting that peptide presentation decisions are not solely dictated by HLA-I affinity (Marijt et al., 2018). The second hypothesis suggests that highly abundant peptides pumped into the ER by TAP may be presented at the expense of less abundant TAP-independent peptides (Oliveira et al., 2011). In line with this hypothesis, boosting TAP-mediated competitor peptide supply into the ER by IFN-γ seemed to decrease TAP-independent SSR1 antigen presentation on wild-type cells. In contrast, a reduction in competitor peptide abundance by depleting TAP from wild-type cells failed to enhance SSR1 peptide presentation, suggesting that also other factors play a role. Because the general abundance of TAP-dependent peptides positively correlates with the expression level of TAP (Boegel et al., 2018; Durgeau et al., 2011), the presentation of TAP-independent peptides may be more efficient on cells with low TAP expression, as long as sufficient peptide-receptive HLA-I heavy chains are available. Thus, presentation of a putative TAP-independent target antigen depends at least on the expression of the antigen-containing protein, TAP and the restricted HLA-I allele, on its affinity and on the amount of competitor peptides. Therefore, safe TAP-independent clinical target definition requires assessment of a broad panel of resting and inflamed healthy cells, including cells
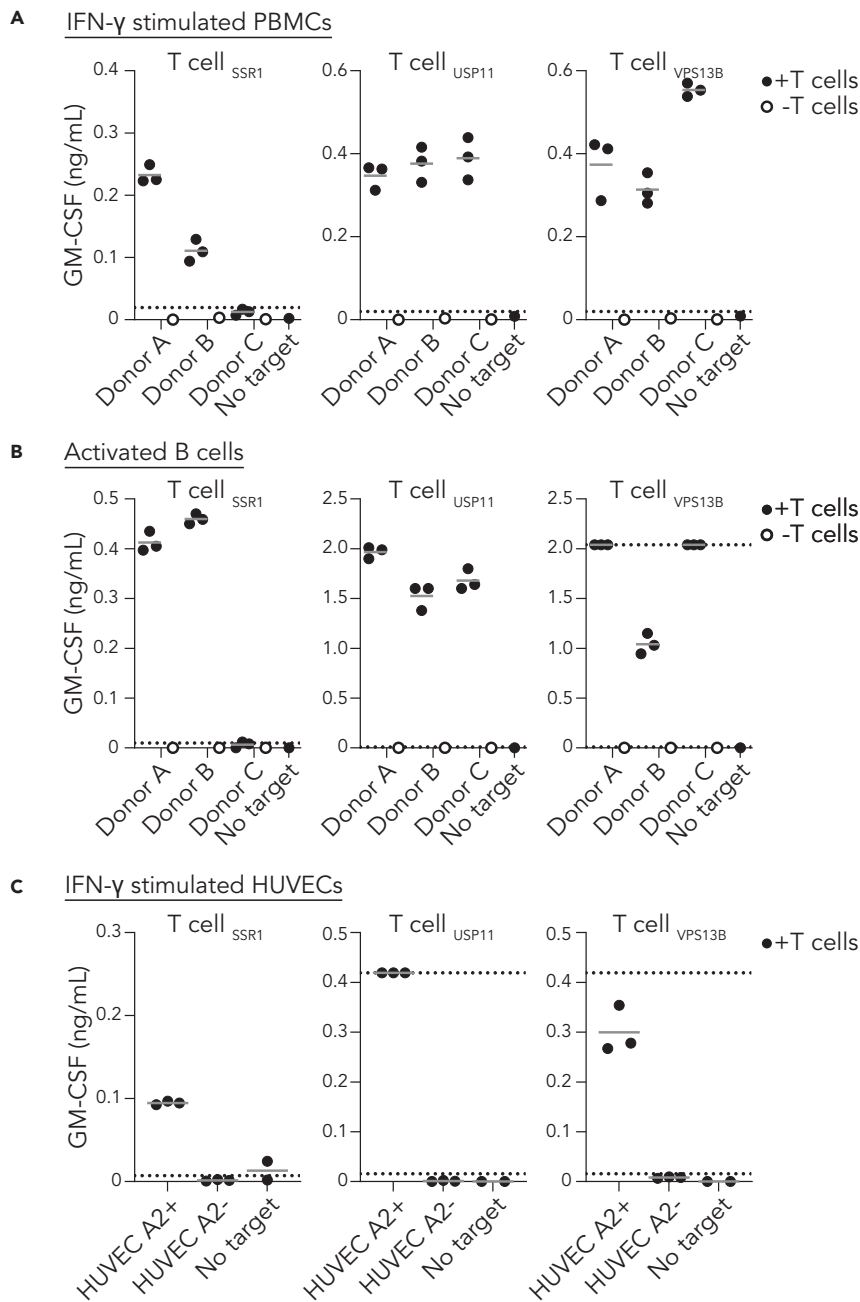
Figure 5. Activated healthy cells functionally present TAP-independent peptides

(A) T cell coculture with healthy donor PBMCs activated for 3 days with IFN-γ.

(B) T cell coculture with healthy donor B cells activated using CpG and B cell receptor cross-linking antibodies.

(C) T cell coculture with HLA-A2 positive and negative HUVECS activated with IFN-γ. Culture supernatants were analyzed using GM-CSF ELISA. Results from triplicate cultures are shown. Dotted lines represent lower and upper detection limit of the ELISAs.

See also Figure S4.

with differential TAP and antigen-encoding gene expression. Activated B cells upregulate HLA-I presentation upon TLR9 stimulation, for example, by CpG (Jiang et al., 2011). These activated B cells prove to be efficient stimulators of CD8^{+} T cells, as demonstrated in Figure 5B, and can be considered for such a panel. In addition, other PBMC-derived cells and HUVECS can be included but also other healthy human cells

such as but not limited to fibroblasts, keratinocytes, melanocytes, differentiated induced pluripotent stem cells or organoids from different organs.

Taken together, the TAP-independent, polymorphic SSR1 antigen provides opportunities to improve our understanding of TAP-independent peptide presentation through T cell- and MS-based experiments on healthy and TAP-deficient cells. Our data warrant testing presentation of candidate TAP-independent target antigens on a broad panel of healthy cells before clinical application.

Limitations of the study

Although we provide a direct proof of principle of TAP-independent antigen presentation by TAP-proficient cells, we have only tested a limited number of healthy donor-derived cells. Panels focusing on validating TAP-independent antigens for immunotherapy should rely on a broader panel of cell types derived from other vital tissues and organs. A technical limitation of this study is that none of the obtained TAP1 KO clones had a frameshifting mutation on both chromosomes. Although we showed absence of TAP1 by immunoblot (de Waard et al., 2020), a decrease in surface HLA-I, and a lack of presentation of cytosolic antigens, we cannot rule out residual TAP function in our model cells. The facts that the peptide is derived from a signal sequence in the ER, and that we and others eluted the SSR1 peptide from TAP-deficient T2 and 721.174 cell lines, respectively (Weinzierl et al., 2008), provide further support of the TAP-independence of the SSR1 antigen.

Resource availability

Lead contact

Further requests for resources and materials should be directed to and will be fulfilled by the lead contact, Robbert M. Spaapen (r.spaapen@sanquin.nl).

Materials availability

TAP1 KO HAP1 cells generated in this study are available from the lead contact with a completed Materials Transfer Agreement.

Data and code availability

Data of peptidome analyses generated in this manuscript are available from the lead contact on request.

METHODS

All methods can be found in the accompanying Transparent methods supplemental file.

SUPPLEMENTAL INFORMATION

Supplemental information can be found online at https://doi.org/10.1016/j.isci.2021.102051.

ACKNOWLEDGMENTS

AUTHORS CONTRIBUTION

Conceptualization and design: A.W. and R.S.; Data acquisition, analysis, and interpretation: A.W., T.V., K.H., D.S., M.J., S.B., D.M.K., A.R., R.S.; Resources and discussion: M.G., M.H., A.A., P.V., R.S.; Supervision and conceptual discussion: R.S.; Writing: A.W., R.S.; Editing: A.W., T.V. and R.S.

DECLARATION OF INTEREST

The authors declare no competing interests.

REFERENCES

Amir, A.L., van der Steen, D.M., Hagedoorn, R.S., Kester, M.G.D., van Bergen, C.A.M., Drijfhout, J.W., de Ru, A.H., Falkenburg, J.H.F., van Veelen, P.A., and Heemskerk, M.H.M. (2011). Allo-HLA–reactive T cells inducing graft-versus-host disease are single peptide specific. Blood 118, 6733–6742.

Bijen, H.M., Hassan, C., Kester, M.G.D., Janssen, G.M.C., Hombrink, P., de Ru, A.H., Drijfhout, J.W., Meiring, H.D., de Jong, A.P., Falkenburg, J.H.F., et al. (2018). Specific T cell responses against minor histocompatibility antigens cannot generally Be explained by absence of their allelic counterparts on the cell surface. Proteomics 18, 1700250.

Boegel, S., Löwer, M., Bukur, T., Sorn, P., Castle, J.C., and Sahin, U. (2018). HLA and proteasome expression body map. BMC Med. Genomics 11, 36.

Brolsma, E. (2019). TEIPP-targeting Immunotherapy Project Funded by Oncode Institute [WWW Document] (Oncode Inst. News.), accessed 1.28.20. https://www.oncode.nl/news/teipp-targeting-immunotherapy-project-funded-by-oncode-institute.

Cameron, B.J., Gerry, A.B., Dukes, J., Harper, J.V., Kannan, V., Bianchi, F.C., Grand, F., Brewer, J.E., Gupta, M., Plesa, G., et al. (2013). Identification of a titin-derived HLA-A1-presented peptide as a cross-reactive target for engineered MAGE A3-directed T cells. Sci. Transl. Med. 5, 197ra103.

Campoli, M., and Ferrone, S. (2008). HLA antigen changes in malignant cells: epigenetic mechanisms and biologic significance. Oncogene 27, 5869–5885.

de Waard, A.A., Verkerk, T., Jongsma, M.L.M., Hoefakker, K., Sethumadhavan, S., Gerke, C., Bliss, S., Kong, X., Janssen, G.M.C., de Ru, A.H., et al. (2020). PAKC: a novel Panel of HLA class I Antigen presentation machinery Knockout Cells from the same genetic origin. Eur. J. Immunol. https://doi.org/10.1002/eji.202048599.

Doorduijn, E.M., Sluijter, M., Marijt, K.A., Querido, B.J., van der Burg, S.H., and van Hall, T. (2018). T cells specific for a TAP-independent self-peptide remain naïve in tumor-bearing mice and are fully exploitable for therapy. Oncoimmunology 7, e1382793.

Doorduijn, E.M., Sluijter, M., Querido, B.J., Oliveira, C.C., Achour, A., Ossendorp, F., van der Burg, S.H., and van Hall, T. (2016). TAP-independent self-peptides enhance T cell recognition of immune-escaped tumors. J. Clin. Invest. 126, 784–794.

Durgeau, A., El Hage, F., Vergnon, I., Validire, P., de Montpréville, V., Besse, B., Soria, J.-C., van Hall, T., and Mami-Chouaib, F. (2011). Different expression levels of the TAP peptide transporter Lead to recognition of different antigenic

peptides by tumor-specific CTL. J. Immunol. 187, 5532–5539.

Gangadhar, T.C., and Vonderheide, R.H. (2014). Mitigating the toxic effects of anticancer immunotherapy. Nat. Rev. Clin. Oncol. 11, 91–99.

Gettinger, S., Choi, J., Hastings, K., Truini, A., Datar, I., Sowell, R., Wurtz, A., Dong, W., Cai, G., Melnick, M.A., et al. (2017). Impaired HLA class I antigen processing and presentation as a mechanism of acquired resistance to immune checkpoint inhibitors in lung cancer. Cancer Discov. 7, 1420–1435.

Hassan, C., Kester, M.G.D., de Ru, A.H., Hombrink, P., Drijfhout, J.W., Nijveen, H., Leunissen, J.A.M., Heemskerk, M.H.M., Falkenburg, J.H.F., and van Veelen, P.A. (2013). The human leukocyte antigen–presented ligandome of B lymphocytes. Mol. Cell. Proteomics 12, 1829–1843.

Hay, K.A., Hanafi, L.-A., Li, D., Gust, J., Liles, W.C., Wurfel, M.M., López, J.A., Chen, J., Chung, D., Harju-Baker, S., et al. (2017). Kinetics and biomarkers of severe cytokine release syndrome after CD19 chimeric antigen receptor–modified T-cell therapy. Blood 130, 2295–2306.

Henden, A.S., and Hill, G.R. (2015). Cytokines in graft-versus-host disease. J. Immunol. 194, 4604–4612.

Jiang, Q., Pan, H., Ye, D., Zhang, P., Zhong, L., and Zhang, Z. (2010). Downregulation of tapasin expression in primary human oral squamous cell carcinoma: association with clinical outcome. Tumor Biol. 31, 451–459.

Jiang, W., Lederman, M.M., Harding, C.V., and Sieg, S.F. (2011). Presentation of soluble antigens to CD8 + T cells by CpG oligodeoxynucleotide-primed human naive B cells. J. Immunol. 186, 2080–2086.

Jongsma, M.L., de Waard, A.A., Raaben, M., Zhang, T., Cabukusta, B., Platzer, R., Blomen, V.A., Xagara, A., Verkerk, T., Bliss, S., et al. (2020). The SPPL3-Defined Glycosphingolipid Repertoire Orchestrates HLA Class I-Mediated Immune Responses. Immunity 54, 132–150.e9, https://doi.org/10.1016/j.immuni.2020.11.003.

Jongsma, M.L.M., Guarda, G., and Spaapen, R.M. (2019). The regulatory network behind MHC class I expression. Mol. Immunol. 113, 16–21.

Kall, L., Krogh, A., and Sonnhammer, E.L.L. (2007). Advantages of combined transmembrane topology and signal peptide prediction–the Phobius web server. Nucleic Acids Res. 35, W429–W432.

Khong, H.T., and Restifo, N.P. (2002). Natural selection of tumor variants in the generation of "tumor escape" phenotypes. Nat. Immunol. 3, 999–1005.

Koike, S., and Jahn, R. (2019). SNAREs define targeting specificity of trafficking vesicles by combinatorial interaction with tethering factors. Nat. Commun. 10, 1608.

Komov, L., Kadosh, D.M., Barnea, E., Milner, E., Hendler, A., and Admon, A. (2018). Cell surface MHC class I expression is limited by the availability of peptide-receptive "empty" molecules rather than by the supply of peptide ligands. Proteomics 18, 1700248.

Ludewig, B., Ochsenbein, A.F., Odermatt, B., Paulin, D., Hengartner, H., and Zinkernagel, R.M. (2000). Immunotherapy with dendritic cells directed against tumor antigens shared with normal host cells results in severe autoimmune disease. J. Exp. Med. 191, 795–804.

Ma, W., Lehner, P.J., Cresswell, P., Pober, J.S., and Johnson, D.R. (1997). Interferon-γ rapidly increases peptide transporter (TAP) subunit expression and peptide transport capacity in endothelial cells. J. Biol. Chem. 272, 16585–16590.

Man, S., Salter, R.D., and Engelhard, V.H. (1992). Role of endogenous peptide in human alloreactive cytotoxic T cell responses. Int. Immunol. 4, 367–375.

Marijt, K.A., Blijleven, L., Verdegaal, E.M.E., Kester, M.G., Kowalewski, D.J., Rammensee, H.-G., Stevanović, S., Heemskerk, M.H.M., van der Burg, S.H., and van Hall, T. (2018). Identification of non-mutated neoantigens presented by TAP-deficient tumors. J. Exp. Med. 215, 2325–2337.

Marijt, K.A., Doorduijn, E.M., and van Hall, T. (2019). TEIPP antigens for T-cell based immunotherapy of immune-edited HLA class IIow cancers. Mol. Immunol. 113, 43–49.

Marijt, K.A., and van Hall, T. (2020). To TAP or not to TAP: alternative peptides for immunotherapy of cancer. Curr. Opin. Immunol. 64, 15–19.

Megger, D.A., Philipp, J., Le-Trilling, V.T.K., Sitek, B., and Trilling, M. (2017). Deciphering of the human interferon-regulated proteome by mass spectrometry-based quantitative analysis reveals extent and dynamics of protein induction and repression. Front. Immunol. 8, 1139.

Morgan, R.A., Chinnasamy, N., Abate-Daga, D., Gros, A., Robbins, P.F., Zheng, Z., Dudley, M.E., Feldman, S.A., Yang, J.C., Sherry, R.M., et al. (2013). Cancer regression and neurological toxicity following anti-MAGE-A3 TCR gene therapy. J. Immunother. 36, 133–151.

Neefjes, J., Jongsma, M.L.M.M., Paul, P., and Bakke, O. (2011). Towards a systems understanding of MHC class i and MHC class II antigen presentation. Nat. Rev. Immunol. 11, 823–836.

Oliveira, C.C., Querido, B., Sluijter, M., de Groot, A.F., van der Zee, R., Rabelink, M.J.W.E., Hoeben,

R.C., Ossendorp, F., van der Burg, S.H., and van Hall, T. (2013). New role of signal peptide peptidase to liberate C-terminal peptides for MHC class I presentation. J. Immunol. *191*, 4020–4028.

Oliveira, C.C., Querido, B., Sluijter, M., Derbinski, J., van der Burg, S.H., and van Hall, T. (2011). Peptide transporter TAP mediates between competing antigen sources generating distinct surface MHC class I peptide repertoires. Eur. J. Immunol. *41*, 3114–3124.

Oliveira, C.C., and van Hall, T. (2015). Alternative antigen processing for MHC class I: multiple roads Lead to rome. Front. Immunol. *6*, 298.

Oliveira, C.C., and van Hall, T. (2013). Importance of TAP-independent processing pathways. Mol. Immunol. *55*, 113–116.

Paul, S., Weiskopf, D., Angelo, M.A., Sidney, J., Peters, B., and Sette, A. (2013). HLA class I alleles are associated with peptide-binding repertoires of different size, affinity, and immunogenicity. J. Immunol. *191*, 5831–5839.

Pfeffer, S., Dudek, J., Schaffer, M., Ng, B.G., Albert, S., Plitzko, J.M., Baumeister, W., Zimmermann, R., Freeze, H.H., Engel, B.D., and Förster, F. (2017). Dissecting the molecular organization of the translocon-associated protein complex. Nat. Commun. *8*, 14516.

Pont, M.J., Oostvogels, R., van Bergen, C.A.M., van der Meijden, E.D., Honders, M.W., Bliss, S., Jongsma, M.L.M., Lokhorst, H.M., Falkenburg, J.H.F., Mutis, T., et al. (2019). T cells specific for an unconventional natural antigen fail to recognize leukemic cells. Cancer Immunol. Res. *7*, 797–804.

Restifo, N.P., Marincola, F.M., Kawakami, Y., Taubenberger, J., Yannelli, J.R., and Rosenberg, S.A. (1996). Loss of functional beta2-microglobulin in metastatic melanomas from five patients receiving immunotherapy. J. Natl. Cancer Inst. *88*, 100–108.

Riemer, A.B., Keskin, D.B., and Reinherz, E.L. (2012). Identification and validation of reference genes for expression studies in human keratinocyte cell lines treated with and without interferon-γ - a method for qRT-PCR reference gene determination. Exp. Dermatol. *21*, 625–629.

Rock, K.L., Reits, E., and Neefjes, J. (2016). Present Yourself! By MHC class I and MHC class II molecules. Trends Immunol. *37*, 724–737.

Rusinova, I., Forster, S., Yu, S., Kannan, A., Masse, M., Cumming, H., Chapman, R., and Hertzog, P.J. (2012). INTERFEROME v2.0: an updated database of annotated interferon-regulated genes. Nucleic Acids Res. *41*, D1040–D1046.

Sade-Feldman, M., Jiao, Y.J., Chen, J.H., Rooney, M.S., Barzily-Rokni, M., Eliane, J.-P.P., Bjorgaard, S.L., Hammond, M.R., Vitzthum, H., Blackmon, S.M., et al. (2017). Resistance to checkpoint blockade therapy through inactivation of antigen presentation. Nat. Commun. *8*, 1136.

Schrodt, S., Koch, J., and Tampé, R. (2006). Membrane topology of the transporter associated with antigen processing (TAP1) within an assembled functional peptide-loading complex. J. Biol. Chem. *281*, 6455–6462.

Shraibman, B., Barnea, E., Kadosh, D.M., Haimovich, Y., Slobodin, G., Rosner, I., López-Larrea, C., Hilf, N., Kuttruff, S., Song, C., et al. (2019). Identification of tumor antigens among the HLA peptidomes of glioblastoma tumors and plasma. Mol. Cell. Proteomics *18*, 1255–1268.

Spaapen, R., van den Oudenalder, K., Ivanov, R., Bloem, A., Lokhorst, H., and Mutis, T. (2007). Rebuilding human leukocyte antigen class II-restricted minor histocompatibility antigen specificity in recall antigen-specific T cells by adoptive T cell receptor transfer: implications for adoptive immunotherapy. Clin. Cancer Res. *13*, 4009–4015.

Spaapen, R.M., Lokhorst, H.M., van den Oudenalder, K., Otterud, B.E., Dolstra, H., Leppert, M.F., Minnema, M.C., Bloem, A.C., and Mutis, T. (2008). Toward targeting B cell cancers with CD4+ CTLs: identification of a CD19-encoded minor histocompatibility antigen using a novel genome-wide analysis. J. Exp. Med. *205*, 2863–2872.

Sultan, H., Trillo-Tinoco, J., Rodriguez, P., and Celis, E. (2017). Effective antitumor peptide vaccines can induce severe autoimmune pathology. Oncotarget *8*, 70317–70331.

Takaba, H., and Takayanagi, H. (2017). The mechanisms of T cell selection in the thymus. Trends Immunol. *38*, 805–816.

Uhlen, M., Fagerberg, L., Hallstrom, B.M., Lindskog, C., Oksvold, P., Mardinoglu, A., Sivertsson, A., Kampf, C., Sjostedt, E., Asplund, A., et al. (2015). Tissue-based map of the human proteome. Science *347*, 1260419.

Van Bergen, C.A.M., Rutten, C.E., Van Der Meijden, E.D., Van Luxemburg-Heijs, S.A.P., Lurvink, E.G.A., Houwing-Duistermaat, J.J., Kester, M.G.D., Mulder, A., Willemze, R., Falkenburg, J.H.F., and Griffioen, M. (2010). High-throughput characterization of 10 new minor histocompatibility antigens by whole genome association scanning. Cancer Res. *70*, 9073–9083.

van der Lee, D.I., Reijmers, R.M., Honders, M.W., Hagedoorn, R.S., de Jong, R.C., Kester, M.G., van der Steen, D.M., de Ru, A.H., Kweekel, C., Bijen, H.M., et al. (2019). Mutated nucleophosmin 1 as immunotherapy target in acute myeloid leukemia. J. Clin. Invest. *129*, 774–785.

van Hall, T., Wolpert, E.Z., van Veelen, P., Laban, S., van der Veer, M., Roseboom, M., Bres, S., Grufman, P., de Ru, A., Meiring, H., et al. (2006). Selective cytotoxic T-lymphocyte targeting of tumor immune escape variants. Nat. Med. *12*, 417–424.

Voldby Larsen, M., Nielsen, M., Weinzierl, A., and Lund, O. (2006). TAP-independent MHC class I presentation. Curr. Immunol. Rev. *2*, 233–245.

Weinzierl, A.O., Rudolf, D., Hillen, N., Tenzer, S., van Endert, P., Schild, H., Rammensee, H.-G., and Stevanović, S. (2008). Features of TAP-independent MHC class I ligands revealed by quantitative mass spectrometry. Eur. J. Immunol. *38*, 1503–1510.

Yee, C., Thompson, J.A., Roche, P., Byrd, D.R., Lee, P.P., Piepkorn, M., Kenyon, K., Davis, M.M., Riddell, S.R., and Greenberg, P.D. (2000). Melanocyte destruction after antigen-specific immunotherapy of melanoma. J. Exp. Med. *192*, 1637–1644.

Zhou, Z., Luo, A., Shrivastava, I., He, M., Huang, Y., Bahar, I., Liu, Z., and Wan, Y. (2017). Regulation of XIAP turnover reveals a role for USP11 in promotion of tumorigenesis. EBioMedicine *15*, 48–61.

Supplemental Information

Healthy cells functionally present

TAP-independent SSR1 peptides: implications

for selection of clinically relevant antigens

Antonius A. de Waard, Tamara Verkerk, Kelly Hoefakker, Dirk M. van der Steen, Marlieke L.M. Jongsma, Dganit Melamed Kadosh, Sophie Bliss, Arnoud H. de Ru, Arie Admon, Peter A. van Veelen, Marieke Griffioen, Mirjam H.M. Heemskerk, and Robbert M. Spaapen

Figure S1
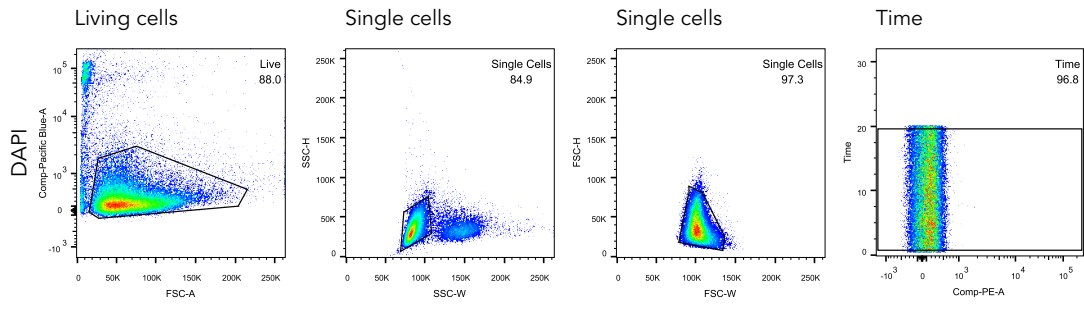
Figure S1. Gating strategy for flow cytometry (Related to Figures 1, 3 and 4)

For all flow cytometric analyses, live cells were gated on DAPI negativity followed by two gates for single cells using SSC-H vs SSC-W and FSC-H vs FSC-W. Lastly, any potential artifacts induced by clogs were excluded from analysis by gating on time vs PE.

A

```
WT       /105bp/ GGG ACA GTA CTG CTA CTT CTC GCC GAC TGG GTG CTG CTC CGG ACC GCG CTG CCC CGC ATA TTC TCC
#1       /-----/ --- --- --- --- --- --- --- --- TGC TGG GTG CTG CTC CGG ACC GCG CTG CCC CGC ATA TTC TCC -129bp
#2  chr A         GGG ACA GTA CTG CTA CTT CTC GC- --C TGG GTG CTG CTC CGG ACC GCG CTG CCC CGC ATA TTC TCC -3bp
    chr B         GGG ACA GTA CTG --- --- --- -- CGA CTG GGT GCT GCT CCG GAC CGC GCT GCC CCG CAT ATT CTCC -11bp
#28            GGG ACA GTA CTG C-- --- --- --- --- --- --- --- -TC CGG ACC GCG CTG CCC CGC ATA TTC TCC -24bp
#34            GGG ACA --- --- --- --- --- --- --- --- GTG CTG CTC CGG ACC GCG CTG CCC CGC ATA TTC TCC -24bp
#37  chr A       GGG ACA GTA CTG CTA CTT CTC GCT --- --- --- --- --- --- ACC GCG CTG CCC CGC ATA TTC TCC -18bp
     chr B       GGG ACA GTA CTG CTA CTT CT- --- --- --- -T GCT GCT CCG GAC CGC GCT GCC CCG CAT ATT CTCC -11bp
```

TAP1 gRNA   PAM site
– Deletions   Stop codon
Substitution

B

```
        40         50         60         70         80         90        100        110
WT    RPHRGAESPRPGRDRDGVRVPMASSRCPAPRGCRCLPGASLAWLGTVLLLLADWVLLRTALPRIFSLLVPTA
#1    RPHRGAESP-----------------------------------------------CWVLLRTALPRIFSLLVPTA -43aa
#2    RPHRGAESPRPGRDRDGVRVPMASSRCPAPRGCRCLPGASLAWLGTVLLLLA-WVLLRTALPRIFSLLVPTA -1aa
#28   RPHRGAESPRPGRDRDGVRVPMASSRCPAPRGCRCLPGASLAWLGTVL--------LRTALPRIFSLLVPTA -8aa
#34   RPHRGAESPRPGRDRDGVRVPMASSRCPAPRGCRCLPGASLAWLGT--------VLLRTALPRIFSLLVPTA -8aa
#37   RPHRGAESPRPGRDRDGVRVPMASSRCPAPRGCRCLPGASLAWLGTVLLLLA------TALPRIFSLLVPTA -6aa
```

– Deletions
Transmembrane domain
Substitution

C

Figure S2. HAP1 TAP1 KO clone characteristics (Related to Figure 1)

(**A**) Summary of TAP1 gene editing in each TAP1 KO clone. Indicated are the gRNA targeting sequence (blue) with PAM site (green), insertions (red), deletions (dashes) and premature stop codons (orange). Clone #1 was previously described (de Waard et al., 2020). (**B**) Summary of the targeted part of the TAP1 amino acid sequence with the genome editing result depicted for each clone. Numbers above the sequence indicate the amino acid location in the wild type TAP1 protein. Transmembrane domain in wild type sequence (blue), amino acids lacking in TAP1 KO clones (dashes) and amino acid substitutions (red) are depicted. (**C**) Correlation analysis of HLA-A2 expression of HAP1 TAP1 KO clones (geometric mean fluorescent intensity, Figure 1C) with their capacity to activate SSR1-specific T cell response (Figure 1D).

Figure S3

SSR1 (284 amino acids)

MRLLPRLLLLLLLLVFPAT**VLFRGGPRG(S/L)LAVA**QDLTEDEETVEDSIIEDEDDEAEVEEEPDLVEDKEEEDVSGEPEASPSADTTILFVKGEDFPANNIV
KFLVGFTNKGTEDFIVESLDASFRYPQDYQFYIQNFTALPLNTVVPPQRQATFEYSFIPAEPMGGRPFGLVINLNYKDLNGNVFQDAVFNQTVTVIEREDGLD
GETIFMYMFLAGLGLLVIVGLHQL*LESRKRKRPIQKVEMGTSSQNDVDMSWIPQETLNQINKASPRRLPRKRAQKRSVGSDE*

* (above VLFRGGPRG(S/L)LAVA region)

<u>Signal peptide</u>
Recognized antigen *nonsynonymous SNP rs10004
Peptides identified by MS
Transmembrane domain
Cytosolic domain

Figure S3. Amino acid sequence and features of SSR1 (Related to Figure 2)

The location of the peptide recognized by the SSR1-specific T cell clone is depicted in red with the asterisk indicating the SNP (rs10004). The predicted signal peptide is underlined, the predicted transmembrane domain orange and the cytosolic domain in italics. Peptides eluted from various HLA-I alleles (Table S3) are depicted in green.

A Fresh PBMCs

● +T cells
○ -T cells

T cell SSR1, T cell USP11, T cell VPS13B — IFN-γ (ng/mL) vs Donor A, Donor B, Donor C, No target

B Monocytes

● +T cells
○ -T cells

T cell SSR1, T cell USP11, T cell VPS13B — IFN-γ (ng/mL) vs Donor A, Donor B, Donor C, No target

C HUVECs

T cell SSR1, T cell USP11, T cell VPS13B — IFN-γ (ng/mL) vs HUVEC A2+, HUVEC A2-, No target

D HUVECs

●— HUVEC A2+
■— HUVEC A2-

T cell SSR1, T cell USP11 — Specific lysis (%) vs T cell: target ratio (1:1, 5:1, 25:1)

E Activated B cells

●— Donor A
■— Donor B
▲— Donor C

T cell SSR1, T cell USP11 — Specific lysis (%) vs T cell: target ratio (1:1, 5:1, 25:1)
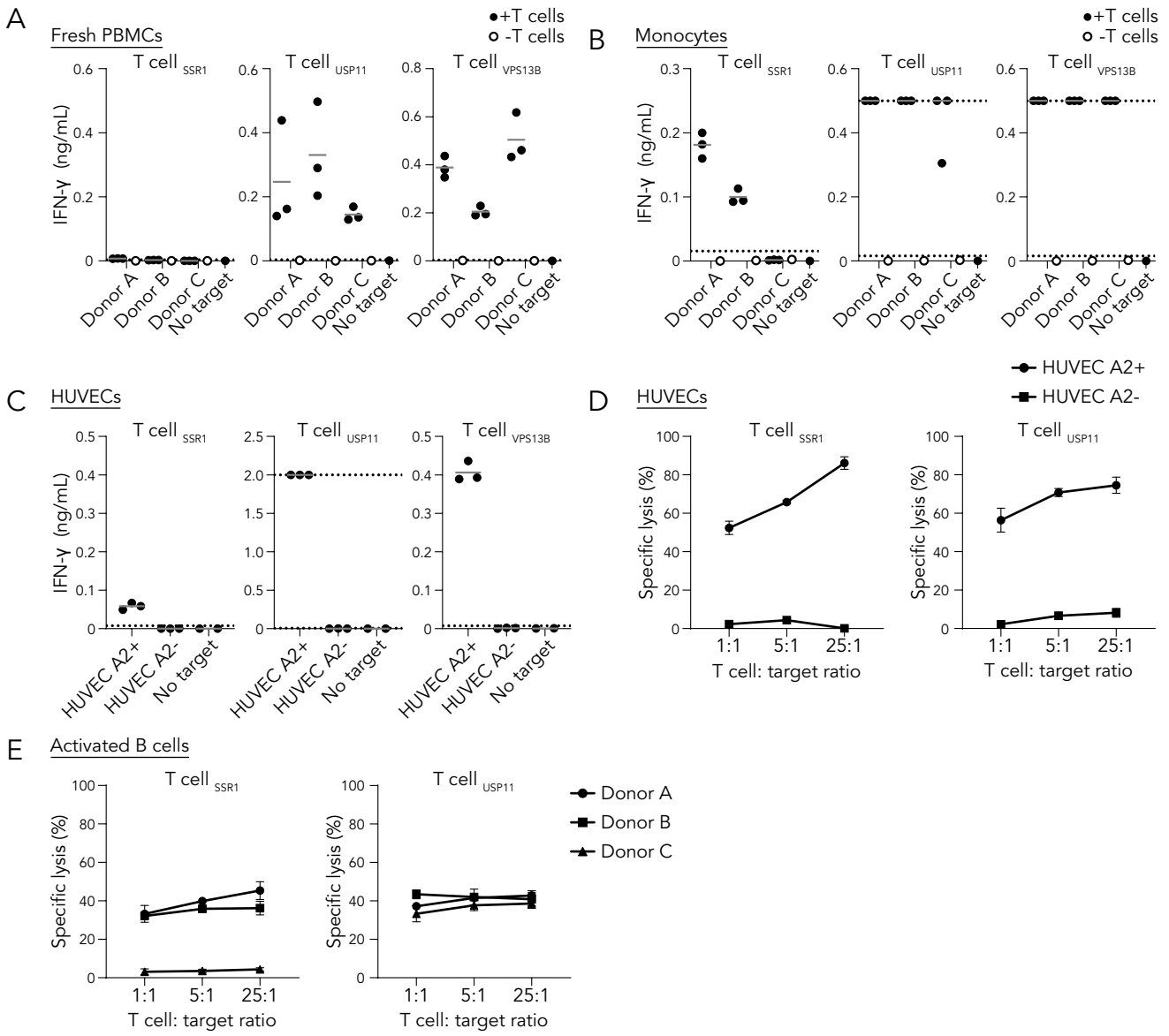
Figure S4. Specific recognition and lysis of multiple healthy cell types (Related to Figures 3 and 5)

(**A**) T cell coculture with PBMCs from three healthy donors (see Figure 3B), culture supernatant was analyzed by IFN-γ ELISA (GM-CSF in Figure 3). Results from triplicate cultures are shown. Dotted lines represent the detection limits of the ELISA. (**B**) As in (A) but using monocytes as target cells (GM-CSF in Figure 3). (**C**) T cell coculture with HLA-A2 positive and negative HUVECs (see Figure 3F). Culture supernatant was analyzed by IFN-γ ELISA (GM-CSF in Figure 3). Each dot represents an individual measurement of triplicate cultures. (**D** and **E**) The indicated T cells were cocultured with ^{51}Cr-loaded (**D**) HLA-A2 positive or negative HUVECs (see Figure 3F) or (**E**) B cells isolated from three healthy donors (see Figure 3B) activated using CpG and B cell receptor crosslinking antibodies at indicated effector:target cell ratios. Specific lysis (%) was calculated based on the ^{51}Cr release. Each datapoint represents the mean of triplicate cultures with SD.

Table S1. All theoretical 8-14mer peptides covering the SSR1 SNP (Related to Tables 1 and 2)

Affinities for HLA-A*02:01 of all theoretical SSR1-derived peptides covering the nonsynonymous SNP rs10004 predicted using NetMHC4.0.

Peptide sequence	Predicted affinity for HLA-A*02:01 (nM) per variant	
	L	S
FRGGPRGL	36658	43601
RGGPRGLL	39127	41929
GGPRGLLA	38138	43187
GPRGLLAV	26994	33459
PRGLLAVA	35607	39522
RGLLAVAQ	34391	37964
GLLAVAQD	27129	40492
LLAVAQDL	6903	10021
LFRGGPRGL	30649	39466
FRGGPRGLL	31365	34114
RGGPRGLLA	29547	36909
GGPRGLLAV	16626	23894
GPRGLLAVA	26057	30604
PRGLLAVAQ	34960	38808
RGLLAVAQD	32556	35998
GLLAVAQDL	286	13769
LLAVAQDLT	5043	5748
VLFRGGPRGL	777	16308
LFRGGPRGLL	33415	35308
FRGGPRGLLA	26878	36619
RGGPRGLLAV	16823	23776
GGPRGLLAVA	26366	33402
GPRGLLAVAQ	32540	36539
PRGLLAVAQD	37729	40484
RGLLAVAQDL	1447	20810
GLLAVAQDLT	2684	18948
LLAVAQDLTE	21253	23246
TVLFRGGPRGL	7427	30851
VLFRGGPRGLL	4673	5524
LFRGGPRGLLA	32850	38768
FRGGPRGLLAV	18430	25942
RGGPRGLLAVA	29760	35464
GGPRGLLAVAQ	34513	38438
GPRGLLAVAQD	36423	39518
PRGLLAVAQDL	8766	30236
RGLLAVAQDLT	11515	29918

Table S1 (continued)

Peptide sequence	L	S
GLLAVAQDLTE	15158	31575
LLAVAQDLTED	32609	34026
ATVLFRGGPRGL	8580	31521
TVLFRGGPRGLL	6482	7682
VLFRGGPRGLLA	5795	10082
LFRGGPRGLLAV	20279	27386
FRGGPRGLLAVA	23552	30074
RGGPRGLLAVAQ	32152	36590
GGPRGLLAVAQD	35448	39262
GPRGLLAVAQDL	7843	30371
PRGLLAVAQDLT	13387	30950
RGLLAVAQDLTE	15461	31263
GLLAVAQDLTED	16550	34127
LLAVAQDLTEDE	33202	34697
PATVLFRGGPRGL	8936	31494
ATVLFRGGPRGLL	7517	8908
TVLFRGGPRGLLA	7199	12668
VLFRGGPRGLLAV	236	628
LFRGGPRGLLAVA	24754	31034
FRGGPRGLLAVAQ	27133	32927
RGGPRGLLAVAQD	33051	37463
GGPRGLLAVAQDL	7960	30542
GPRGLLAVAQDLT	13423	30972
PRGLLAVAQDLTE	17551	31764
RGLLAVAQDLTED	16889	33306
GLLAVAQDLTEDE	17723	35216
LLAVAQDLTEDEE	34948	36072
FPATVLFRGGPRGL	9143	27652
PATVLFRGGPRGLL	7833	9280
ATVLFRGGPRGLLA	7941	14000
TVLFRGGPRGLLAV	351	958
VLFRGGPRGLLAVA	649	1403
LFRGGPRGLLAVAQ	27460	32988
FRGGPRGLLAVAQD	28291	34050
RGGPRGLLAVAQDL	7397	29261
GGPRGLLAVAQDLT	13582	31110
GPRGLLAVAQDLTE	17371	31898
PRGLLAVAQDLTED	19135	33912
RGLLAVAQDLTEDE	17765	34570
GLLAVAQDLTEDEE	18231	35941
LLAVAQDLTEDEET	24639	25997

Table S2. SSR1-derived peptides are presented in the absence and presence of functional TAP (Related to Table 2)

SSR1 candidate peptides were eluted from wild type and TAP-deficient HAP1 cells or wild type MCF-7 cells and MCF-7 cells overexpressing the Herpes Simplex Virus-derived TAP inhibitor ICP47. Values correspond to the average log2-intensity of the LC-MS/MS data. The SADTTILF and SADTTILFV peptides are attributed to HLA-C*05:01 based on binding prediction by NetMHC4.0 (rank<=2).

Peptide	HLA-I allele	HAP1 cells			MCF-7 cells		
		WT	TAP1 KO #1	TAP1 KO #2	WT	ICP47 #C15	ICP47 #C32
SADTTILF	C*05:01	-	-	-	23.5	-	20.9
SADTTILFV	C*05:01	-	-	-	23.8	23.0	22.7
VLFRGGPRGSLAVA	A*02:01	32.5	-	33.1	-	-	-

Table S3. SSR1-derived peptides are presented on various HLA-I alleles (Related to Table 2)

Data derived from (Shraibman et al., 2019) showing SSR1-derived peptides eluted from different glioblastoma and control patients/donors and predicted to bind one or multiple of the patient-expressed HLA-I alleles by NetMHC4.0 (rank<=2).

Patient	Peptide				
	FPANNIVKF	FRYPQDYQF	NYKDLNGNVF	SADTTILFV	TEDFIVESL
11-002	B*35:03	B*35:03 C*12:03	A*24:02		
11-004			A*24:02		
11-006			A*24:02		
29/14					B*40:01
30-002	B*53:01 C*04:01				
50/14			A*24:02		
637/13			A*24:02		
BCN-004	A*26:01				
BCN-017			C*05:01		
BCN-019	C*04:01				
BCN-021			A*24:02		
CPH-07	C*04:01	B*27:05			
CPH-08					B*40:02
CPH-09		B*27:05		C*05:01	
Leiden-003	C*04:01				
Leiden-004				C*12:03	
Leiden-005	A*25:01				
AMRF*	Cw4				
CMLF*	Cw4				
DMRN*	Cw4		A*24:02		
E16*	Cw4				
E27*			A*24		
E45*	Cw4				
E48*	Cw4				
EMMS*	Cw4				
FHCR*			A*24:02		
JGMS[#]			A*24:02		
JHGP[#]			A*23:01		
MRSRCS*			A*24:02		
VSCP[#]			A*24		

*Non-cancerous arthritis control patient.

[#]Non-cancerous healthy control donor.

Transparent Methods

Cell culture

HAP1 (HLA-A*02:01, HLA-B*40:01, HLA-C*03:04), EBV-LCLs, HEK293T, U266, U2G10196, COV413b, T2, UM9, and TMD8 cells were cultured in Iscove's Modified Dulbecco's Medium (IMDM, Gibco and Lonza) supplemented with 10% heat-inactivated fetal calf/bovine serum (Gibco, Thermo Fisher) and antibiotics (PenStrep; Invitrogen; IMDM^{++}) at 37°C and 5% CO_2. MCF-7 (HLA-A*02:01, HLA-B*18:01, HLA-B*44:02, HLA-C*05:01) were cultured in DMEM (Dulbecco's modified Eagle's medium), supplemented with 10% heat-inactivated fetal bovine serum (FBS), 1% L-glutamine, and 1% penicillin- streptomycin, in a humidified 5% CO2 incubator at 37°C. Primary HUVECs (kindly provided by Dr. Jaap van Buul), pooled from three different donors (Lonza), were cultured in Endothelial Cell Growth medium 2 (EGM2, Lonza) complemented with EGM2 Supplement mix (Promocel), 10% fetal calf serum and antibiotics. The HLA-A*02:01 restricted T cell clones were previously described and recognize a peptide derived from the endogenously expressed human proteins USP11, VPS13B or SSR1 (Amir et al., 2011; Van Bergen et al., 2010). The clones were expanded using irradiated feeder cells (mixed PBMCs and EBV-LCLs exposed to 30 Gy and 50 Gy, respectively) in IMDM with 5% fetal calf serum and 5% human serum (Sanquin), supplemented with 120 U/mL IL-2 (Miltenyi and Chiron), 0.8 µg/mL PHA (HA16 Remel™, ThermoFisher) and antibiotics as described (Pont et al., 2019; Spaapen et al., 2007).

PBMC isolation and activation

Blood was withdrawn from 3 HLA-A2 positive healthy volunteers (Sanquin), PBMCs were isolated by Ficoll gradient separation. Monocytes were isolated through plastic-adherence by incubating fresh PBMCs in IMDM^{++} for 1 h at 37°C and 5% CO_2 on culture plastic. B cells were isolated using anti-CD19 Dynabeads and DETACHaBEAD (Invitrogen) according to manufacturer's protocol. B cell were activated by incubating them with 0.1 µM CpG (Invivogen) and 2.5 µg/mL Fab mix (anti-IGA, IgG and IgM, Jackson ImmunoResearch) in B cell medium (RPMI, Gibco; 5% FCS; 1% L-Glutamine, Life Technologies; 0.1% β-mercaptoethanol, Sigma; 20ng/mL human Transferrin, Sigma, in-house depleted for IgG) for 3 days at 37°C and 5% CO_2.

Sequencing

DNA was isolated from full PBMCs and HLA-A2 positively sorted HUVECs using the NucleoSpin Tissue kit (Machery-Nagel) according to manufacturer's protocol. DNA was amplified using Taq DNA-polymerase (VWR) with forward primer TTCTTCGGTGCATTGTAATTG and reverse primer GGGTCAATGAAACCTTTTTCC and

subsequently Sanger sequenced using the forward primer or a sequencing primer GGTGAACTGGGAGATTCTGTT (HUVECs) and BigDye v1.1 (Applied Biosystems).

Genetic engineering

Genome-editing of HAP1 cells and genomic verification was performed as previously described for TAP1 (de Waard et al., 2020). In short, cells were transduced with pL.CRISPR.efs.GFP (Addgene) containing a gRNA targeting TAP1 (ACTGCTACTTCTCGCCGACT). Transduced cells were enriched by FACS sort on GFP positivity and clones were subsequently generated by limiting dilution. The targeted region was sequenced using primer (GCTCCCCATGAGATCAGCTC) after PCR on genomic DNA of single cell-derived clonal cell lines using forward primer (CAGCCTGTTCCTGGGACTTT) and reverse primer (ACTGACAACGAAGGCGGTAG). HLA-I KO HAP1 cells were previously described (Jongsma et al., 2020). The MCF-7 cells were transfected with pcDNA3.1 containing the Herpes Simplex Virus-derived TAP inhibitor ICP47 using PEI reagent (PolyScience, Niles, Illinois) followed by G418 selection. Clones were generated of which two positive clones were selected (C#15, C#32) (Dganit Melamed Kadosh, Alan Frey, Ian Mohr, and Arie Admon, in preparation).

T cell activation assays

50,000 or 40,000 (only for activated B cells) target cells were cocultured with T cells in a 1:1 ratio in IMDM++ for 18 hours as previously described (Spaapen et al., 2008). IFN-γ and GM-CSF release was measured by standard sandwich ELISA (Sanquin and BioLegend, respectively) according to the manufacturer's protocol. For IFN-γ stimulation, target cells were seeded two (HAP1 cells, HUVECs) or three (PBMCs) days prior to the experiment in a culture flask in IMDM++ containing 20 U/mL recombinant human IFN-γ (Peprotech).

T cell-mediated killing assays

Cytotoxicity experiments were performed as previously described (Jongsma et al., 2020). In short, target cells were loaded with 100 µCi ^{51}Cr (HAP1 and HUVEC, Perkin-Elmer) or 200 µCi ^{51}Cr (B cells) for 90 min at 37°C and washed. T cells were cocultured with 5,000 HAP1 cells, 5,000 HUVECs or 10,000 B cells at indicated effector:target (E:T) ratios for 4-6 h after which 30 µL supernatant was harvested, dried and analyzed using a gamma counter (Wallac). A maximum release control was based on 0.1% triton X-100 treatment. A medium only control was used to detect spontaneous release. Specific lysis (%) was calculated using (experimental cpm – spontaneous cpm) / (maximal cpm – spontaneous cpm)] × 100%.

Flow Cytometry

Trypsinized cells were incubated with antibodies W6/32-PerCP-eFluor710 (pan-HLA; eBioscience) or BB7.2-APC (HLA-A2; eBioscience) in PBS for 30 min at 4°C. Stained cells were fixed in PBS containing 1% formaldehyde (Merck) and DAPI (1 µM, Sigma-Aldrich) for direct analysis by flow cytometry. Samples were analyzed on BD flow cytometers (LSRFortessa or LSR-II). FACS data was analyzed using FlowJo (Tree Star, Inc). Gating strategy is shown in Figure S1. The pooled primary HUVECs were incubated with BB7.2-APC antibody for 30 min at 4°C before they were sorted into HLA-A2 positive and negative cell populations in the presence of DAPI (1 µM) on a BD FACSAria II.

Sample collection and HLA-I peptide elution

Peptide elution of the cell lines shown in Table 1 and 2 was performed as outlined previously (Hassan et al., 2013). Prior to cell pellet generation, UM9, and TMD8 were retrovirally transduced with HLA alleles to express HLA-A*02:01 (UM9-A2, TMD8-A2) and magnetic-activated cell sorting (MACS) enriched for nerve growth factor receptor (NGFR) marker gene expression using anti-R-phycoerythrin (PE) microbeads (Miltenyi Biotec, Bergisch Gladbach, Germany). Cell pellets were made of 5 primary acute myeloid leukemias (AML), 4 primary B cell malignancies (ALL, CLL, HCL), 2 primary ovarian carcinoma (1x ascites) and 2 multiple myeloma cell lines (U266 and UM9-A2), 1 DLBCL cell line (TMD8-A2) and the cell lines T2 and HAP1(de Waard et al., 2020). Primary ovarian carcinoma tumor material was first sliced into small pieces. Dead, clotted or non-tumor material was removed, small tumor tissue was put into a C-tube (Miltenyi Biotec) with ice cold buffer without detergent and complete protease inhibitor (Sigma-Aldrich) to prevent protein degradation and dissociated using a gentleMACS (Miltenyi Biotec) procedure until an almost homogenous cell solution. Cells were lysed in 50 mM Tris-HCl, 150 mM NaCl, 5 mM EDTA, and 0.5% Zwittergent 3-12 (pH 8.0) supplemented with complete protease inhibitor and Benzonase (Merck; 125 IU/mL to remove DNA/RNA complexes). After 2 hours of tumbling in lysis buffer at 4°C, cell lysates were centrifuged for 10 min at 1,000 g at 4°C. The supernatant was subsequently centrifuged for 35 min at 13,000 g at 4°C, precleared with Protein A Sepharose CL-4B beads (GE Healthcare Life Sciences), and subjected to an immunoaffinity column with dimethyl pimelimidate-immobilized W6/32 antibody (2-3 mg/ml resin) on Protein A Sepharose CL-4B beads. After flow through of the cell lysate, the column was washed with 5 to 10 column volumes of lysis buffer and 10 mM Tris-HCl (pH 8.0) buffers with 1 M, 120 mM, and no NaCl, bound HLA class I–peptide complexes were eluted from the column and dissociated with 3 to 4 column volumes of 10% acetic acid. Peptides were separated from HLA class I molecules via passage through a 10 kDa membrane (Macrosep Advance Centrifugal Devices with Supor Membrane, Pall Corp.) and freeze-dried.

Fractionation and mass spectrometry (MS) of HLA-class I peptides

Eluted peptide pools were either fractionated by strong cation exchange chromatography (SCX) or by high pH reversed phase fractionation (High pH-RP). SCX fractionation was performed with a homemade 15 cm SCX column (320 µm inner diameter; polysulfoethyl A, 3 µm, Poly LC) run at 4 µL/min. Gradients were run for 10 min at 100% solvent A (100/0.1 water/trifluoroacetic acid v/v), after which a linear gradient started to reach 100% solvent B (65/35/0.1 250 mM KCl/acetonitrile (ACN)/trifluoroacetic acid v/v/v) over 15 min, followed by 100% solvent C (65/35/0.1 500 mM KCl/ACN/trifluoroacetic acid v/v/v) over the next 15 min. The gradient remained at 100% solvent C for 5 min and then switched again to 100% solvent A. Twenty 4 µL fractions were collected in vials prefilled with 20 µL 95/3/0.1 water/ACN/formic acid v/v/v and freeze-dried. High pH-RP fractionation was performed on an Oasis HLB 1cc SPE column (Waters). The column was first equilibrated with 1 mL 10/90 water/ACN v/v, washed 2 times by passing 1 mL of 10 mM ammonium bicarbonate (ambic) buffer pH=8.4 through the column. The freeze-dried peptide mixture was diluted in 10 mM ambic pH 8.4 and gently pushed through the column and washed again with 1 mL of 10 mM ambic pH 8.4. Fractions were taken by steadily increasing the amount of ACN into the elution buffer in the range of 5% to 50% ACN and freeze-dried.

Freeze-dried peptide fractions were dissolved in 95/3/0.1 water/ACN/formic acid v/v/v and analyzed as described previously (van der Lee et al., 2019). The peptides were analyzed by data-dependent MS/MS on a Q Exactive mass spectrometer equipped with an easy-nLC 1000 (Thermo Fisher Scientific) oran LTQ FT Ultra equipped with a nanoflow liquid chromatography 1100 HPLC system (Agilent Technologies). Peptides were trapped at 6–10 µL/min on a 1.5 cm column (100 µm internal diameter; ReproSil-Pur C18-AQ, 3 µm, Dr. Maisch HPLC GmbH) followed by elution to a 20 cm column (50 µm internal diameter; ReproSil-Pur C18-AQ, 3 µm) at 150 nL/min. The column was developed with a 0-40% ACN gradient in 0.1% formic acid for 120 min. The eluent was sprayed into the mass spectrometer by drawing the end of the column to a tip (internal diameter of ~5µm). Full-scan MS spectra were acquired in the FT-ICR with a target value of 3,000,000 at a resolution of 25,000. The 2 most intense ions were isolated for accurate FT-ICR mass measurements by a selected ion monitoring scan with a target accumulation value of 50,000 at a resolution of 50,000followed by fragmentation in the linear ion trap using collision-induced dissociation at a target value of 10,000. The Q Exactive mass spectrometer was used in top10 mode with an AGC target value of 3,000,000/maximum fill time of 20 ms (full scan) at a resolution of 70,000 and an AGC target value of 100,000/maximum fill time of 60 ms for MS/MS at a resolution of 17,500 and an intensity threshold of 17,000. Apex trigger was 1-10 sec with 2-6 allowed charges. The Orbitrap Fusion LUMOS mass spectrometer was used in data-dependent MS/MS (top-N

mode), with recording of the MS2 spectrum in the orbitrap with a collision energy at 32 V. For master scan (MS1), the AGD target was 400,000/maximum fill time of 50 ms at a resolution of 60,000 and scan range 300-1,400. Charge states 1–4 were included and the dynamic exclusion was set after n=1 with a duration of 20 sec. For MS2, precursors were isolated using the quadrupole with an isolation width of 1.2 Da. HCD collision energy was at 32 V, first mass at 110 Da. The MS2 had an AGC target of 50,000/maximum fill time of 100 ms with a resolution of 30,000. To identify peptides and proteins, Proteome Discoverer version 2.1 (Thermo Fisher Scientific) was used with the mascot node for identification in mascot version 2.2.04 with the UniProt Homo Sapiens database (UP000005640; Jan 2015; 67,911 entries). Cysteine modifications were set as variably for Methionine oxidation and cysteinylation. Precursor tolerance of 10 ppm and MS/ MS fragment tolerance of 20 mmu was used for peptide assignment for the Q Exactive data and 2 ppm and 0.5 Da for LTQ FT Ultra data.

The HLA-I peptidome analyses of the HAP1 and MCF7 cells shown in Table S3 were done using exactly the HLA immunoaffinity purification and LC-MS/MS procedures as in Komov et al. 2018 (Komov et al., 2018).

Synthetic peptide stimulation

Synthetic peptides were titrated on 20,000 T2 cells prior to incubation with 5,000 T cells for 18 hours before cytokine ELISA similar as previously described (Bijen et al., 2018).

Expression analysis

Data on SSR1, CD3E, CD14 and CD19 RNA expression in blood cells and of SSR1, CD45 and PECAM1 in HUVECs was retrieved from the Human Protein Atlas (https://www.proteinatlas.org)(Uhlen et al., 2015) using the RNA HPA blood cell gene and the RNA HPA cell line gene datasets. Data for B and T cells was pooled from the different naïve and memory subsets. Microarray data of IFN-γ stimulated human cells were selected based on equal *in vitro* treatment with 200 U/mL IFN-γ for 24 hours containing expression data on SSR1 (downloaded from Interferome.org v2.01, datasets 64, 144, 311). PPIA was selected as house-hold control as it is unaffected by interferon signaling and was present in all datasets (Riemer et al., 2012). VPS13B and USP11 expression was only present in datasets 64 and 144, respectively.

Statistical Analyses

All error bars correspond to the standard deviation of the mean. Statistical evaluations were done by a student's t-test for comparison of two independent groups (T cell assay on HAP1 wild type and TAP1 KO cells), a repeated measures one-way ANOVA followed by Dunnett's

multiple comparisons test for comparison of change in gene expression derived from multiple datasets (IFN-γ regulation of mRNA), an one-way ANOVA followed by Dunnett's multiple comparisons test (IFN-γ regulation of protein) or Sidak's multiple comparisons test (T cell assay on IFN-γ stimulated HAP1 cells) for multigroup analyses with Prism software (www.graphpad.com). Statistical evaluation of primary cell cocultures was unnecessary due to the qualitative goal of the experiments.

Supplemental References

Amir, A.L., van der Steen, D.M., Hagedoorn, R.S., Kester, M.G.D., van Bergen, C.A.M., Drijfhout, J.W., de Ru, A.H., Falkenburg, J.H.F., van Veelen, P.A., Heemskerk, M.H.M., 2011. Allo-HLA–reactive T cells inducing graft-versus-host disease are single peptide specific. Blood 118, 6733–6742.

Bijen, H.M., Hassan, C., Kester, M.G.D., Janssen, G.M.C., Hombrink, P., de Ru, A.H., Drijfhout, J.W., Meiring, H.D., de Jong, A.P., Falkenburg, J.H.F., Jimenez, C.R., Heemskerk, M.H.M., van Veelen, P.A., 2018. Specific T Cell Responses against Minor Histocompatibility Antigens Cannot Generally Be Explained by Absence of Their Allelic Counterparts on the Cell Surface. Proteomics 18, 1700250.

de Waard, A.A., Verkerk, T., Jongsma, M.L.M., Hoefakker, K., Sethumadhavan, S., Gerke, C., Bliss, S., Kong, X., Janssen, G.M.C., de Ru, A.H., Claas, F.H.J., Mulder, A., Tampé, R., van Veelen, P.A., Halenius, A., Spaapen, R.M., 2020. PAKC: A novel Panel of HLA class I Antigen presentation machinery Knockout Cells from the same genetic origin. Eur. J. Immunol. https://doi.org/10.1002/eji.202048599

Hassan, C., Kester, M.G.D., de Ru, A.H., Hombrink, P., Drijfhout, J.W., Nijveen, H., Leunissen, J.A.M., Heemskerk, M.H.M., Falkenburg, J.H.F., van Veelen, P.A., 2013. The Human Leukocyte Antigen–presented Ligandome of B Lymphocytes. Mol. Cell. Proteomics 12, 1829–1843.

Jongsma, M.L., de Waard, A.A., Raaben, M., Zhang, T., Cabukusta, B., Platzer, R., Blomen, V.A., Xagara, A., Verkerk, T., Bliss, S., Kong, X., Gerke, C., Janssen, L., Stickel, E., Holst, S., Plomp, R., Mulder, A., Ferrone, S., Claas, F.H., Heemskerk, M.H., Griffioen, M., Halenius, A., Overkleeft, H., Huppa, J.B., Wuhrer, M., Brummelkamp, T.R., Neefjes, J., Spaapen, R., 2020. The SPPL3-Defined Glycosphingolipid Repertoire Regulates Immune Responses by Improving HLA Class I Access. Immunity. https://doi.org/10.1016/j.immuni.2020.11.003

Komov, L., Kadosh, D.M., Barnea, E., Milner, E., Hendler, A., Admon, A., 2018. Cell Surface MHC Class I Expression Is Limited by the Availability of Peptide-Receptive "Empty" Molecules Rather than by the Supply of Peptide Ligands. Proteomics 18, 1700248.

Pont, M.J., Oostvogels, R., van Bergen, C.A.M., van der Meijden, E.D., Honders, M.W., Bliss, S., Jongsma, M.L.M., Lokhorst, H.M., Falkenburg, J.H.F., Mutis, T., Griffioen, M., Spaapen, R.M., 2019. T Cells Specific for an Unconventional Natural Antigen Fail to Recognize Leukemic Cells. Cancer Immunol. Res. 7, 797–804.

Riemer, A.B., Keskin, D.B., Reinherz, E.L., 2012. Identification and validation of reference genes for expression studies in human keratinocyte cell lines treated with and without interferon-γ - a method for qRT-PCR reference gene determination. Exp. Dermatol. 21, 625–629.

Shraibman, B., Barnea, E., Kadosh, D.M., Haimovich, Y., Slobodin, G., Rosner, I., López-Larrea, C., Hilf, N., Kuttruff, S., Song, C., Britten, C., Castle, J., Kreiter, S., Frenzel, K.,

Tatagiba, M., Tabatabai, G., Dietrich, P.-Y., Dutoit, V., Wick, W., Platten, M., Winkler, F., von Deimling, A., Kroep, J., Sahuquillo, J., Martinez-Ricarte, F., Rodon, J., Lassen, U., Ottensmeier, C., van der Burg, S.H., Thor Straten, P., Poulsen, H.S., Ponsati, B., Okada, H., Rammensee, H.-G., Sahin, U., Singh, H., Admon, A., 2019. Identification of Tumor Antigens Among the HLA Peptidomes of Glioblastoma Tumors and Plasma. Mol. Cell. Proteomics 18, 1255–1268.

Spaapen, R., van den Oudenalder, K., Ivanov, R., Bloem, A., Lokhorst, H., Mutis, T., 2007. Rebuilding Human Leukocyte Antigen Class II-Restricted Minor Histocompatibility Antigen Specificity in Recall Antigen-Specific T Cells by Adoptive T Cell Receptor Transfer: Implications for Adoptive Immunotherapy. Clin. Cancer Res. 13, 4009–4015.

Spaapen, R.M., Lokhorst, H.M., van den Oudenalder, K., Otterud, B.E., Dolstra, H., Leppert, M.F., Minnema, M.C., Bloem, A.C., Mutis, T., 2008. Toward targeting B cell cancers with CD4+ CTLs: identification of a CD19-encoded minor histocompatibility antigen using a novel genome-wide analysis. J. Exp. Med. 205, 2863–2872.

Uhlen, M., Fagerberg, L., Hallstrom, B.M., Lindskog, C., Oksvold, P., Mardinoglu, A., Sivertsson, A., Kampf, C., Sjostedt, E., Asplund, A., Olsson, I., Edlund, K., Lundberg, E., Navani, S., Szigyarto, C.A.-K., Odeberg, J., Djureinovic, D., Takanen, J.O., Hober, S., Alm, T., Edqvist, P.-H., Berling, H., Tegel, H., Mulder, J., Rockberg, J., Nilsson, P., Schwenk, J.M., Hamsten, M., von Feilitzen, K., Forsberg, M., Persson, L., Johansson, F., Zwahlen, M., von Heijne, G., Nielsen, J., Ponten, F., 2015. Tissue-based map of the human proteome. Science (80-.). 347, 1260419–1260419.

Van Bergen, C.A.M., Rutten, C.E., Van Der Meijden, E.D., Van Luxemburg-Heijs, S.A.P., Lurvink, E.G.A., Houwing-Duistermaat, J.J., Kester, M.G.D., Mulder, A., Willemze, R., Falkenburg, J.H.F., Griffioen, M., 2010. High-Throughput Characterization of 10 New Minor Histocompatibility Antigens by Whole Genome Association Scanning. Cancer Res. 70, 9073–9083.

van der Lee, D.I., Reijmers, R.M., Honders, M.W., Hagedoorn, R.S., de Jong, R.C., Kester, M.G., van der Steen, D.M., de Ru, A.H., Kweekel, C., Bijen, H.M., Jedema, I., Veelken, H., van Veelen, P.A., Heemskerk, M.H., Falkenburg, J.H.F., Griffioen, M., 2019. Mutated nucleophosmin 1 as immunotherapy target in acute myeloid leukemia. J. Clin. Invest. 129, 774–785.